THE UNIVERSITY OF ALBERTA

A STUDY OF UPCONVERSION PHENOMENA IN IMPATT-AMPLIFIERS

BY

© RAMESH K. GUPTA

A THESIS

SUBMITTED TO THE FACULTY OF GRADUATE STUDIES AND RESEARCH

IN PARTIAL FULFILMENT OF THE REQUIREMENT FOR THE

DEGREE OF MASTER OF SCIENCE IN ELECTRICAL ENGINEERING

DEPARTMENT OF ELECTRICAL ENGINEERING

EDMONTON, ALBERTA

FALL, 1976

ABSTRACT

Microwave upconversion in Impatt-amplifiers can be achieved by impressing the baseband (i.f.) signal on the bias circuit of the amplifier. Relatively large conversion gain can be obtained by use of such a scheme. A theoretical as well as experimental study of the conversion process in Impatt-amplifiers has been made.

Theoretical analysis for small i.f. signals, based on admittance characteristics of the device and the circuit has been done. It was expected that sideband generation would be due predominently to the gain magnitude variations with the applied i.f. signal. Conversion characteristics are predicted to be similar to amplifier characteristics. A conversion gain of 5dB at small signal i.f. is predicted which is expected to increase for increasing i.f. levels.

Experimental results obtained for two Impatt-amplifiers are in good qualitative agreement with the theory. A maximum conversion gain of 13d was obtained. The results indicate that there is a shift in admittance characteristics of the device with increased i.f. levels. Results also show that the response of microwave circuits at component frequencies plays an important role in determining converter response. Some sideband generation due to frequency (phase) modulation of the r.f. is also observed.

An experimental investigation of the distortion introduced by the conversion process, using amplitude modulation of the i.f., shows that the second harmonic is always more than 30dB below the fundamental.

ACKNOWLEDGEMENT

I wish to express my sincere thanks to Dr. Colin G. Englefield, my thesis supervisor, for his invaluable help and encouragement during the course of this work. I am very thankful to Dr. A. Javed for many helpful discussions and suggestions. To B. Syrett and N. Mansour, fellow graduate students in the Microwave Electronics Laboratory, I am thankful for their co-operation, encouragement and understanding.

I owe special thanks to Mr. Jim Fearn for his technical assistance in the experimental work.

To Dr. J. Nigrin and the Departmental Workshop staff, I am thankful for their assistance in design and construction of the amplifiers. I wish to thank Mrs. Barbara J. Gallaiford for expert and excellent typing of the manuscript.

Graduate Assistance and Intersession bursaries provided by the Department of Electrical Engineering and the University of Alberta are gratefully acknowledged.

I am always indebted to my parents, members of my parental family and all my friends for their continuous encouragement and moral support.

TABLE OF CONTENTS

LIST OF TABLES

LIST OF FIGURES

LIST OF SYMBOLS

$\tilde{d}$ - Variations in the denominator vector

$\tilde{n}$ - Variations in the numerator vector

ω_1 - Baseband or intermediate frequency

ω_p - Microwave pump frequency

$\vec{D}$ - Denominator vector in the gain expression

$\vec{N}$ - Numerator vector in the gain expression

P - Amplifier power gain

$V_{i.f.}$ - Intermediate frequency voltage

V_{in} - Input microwave voltage

V_{out} - Output microwave voltage

Y_D - Device admittance at the diode wafer

Y_L - Circuit admittance

$\tilde{Y}_d$ - Device admittance variations

Y_{d_n} - nth order admittance variations

β - Ratio of first order admittance variations Y_{d_1} and the denominator scalar

Γ - Reflection coefficient of the amplifier

ϕ - Phase shift in the amplifier

CHAPTER 1

INTRODUCTION

Frequency upconverters play a very important role in microwave communication systems. In heterodyne relay and radar systems, the intermediate frequency (i.f.) is mixed with a microwave local oscillator frequency in an upconverter to obtain the modulated microwave signal. This signal is then transmitted after power amplification. Microwave upconverters in general, can be classified into two categories, employing either of the following properties:

1. The non-linear capacitance of devices such as varactor diodes.
2. The non-linear negative resistance of active devices.

According to the Manley and Rowe theory, in nonlinear capacitance upconverters, it is theoretically possible to have a conversion gain equal to the ratio of output to input frequency. In practice, however, there is a conversion loss of a few dB and the losses introduced by varactor diodes increase significantly at higher frequencies in the microwave range. Much higher conversion gains can be obtained using negative resistance upconverters at almost all frequencies in the microwave region.

With the advent of solid state microwave sources in recent years and their successful use as oscillators and amplifiers, the second method deserves careful analysis and investigation. Out of all the solid-state microwave devices presently available, Impatt diodes are well recognised as relatively high power devices and are being put into use in communication systems. Impatt oscillators, when used as upconverters,

have a definite advantage over Impatt-amplifiers in that they are "self-pumped." However, they are normally unstable in frequency. Because of the considerations outlined above, the work described in this thesis is confined to the study of frequency conversion effects in Impatt-amplifiers.

1.1 Historical Background:

The generation of microwave power in a reverse biased p-n junction was originally suggested by Read [19] in 1958. It was not until 1965 when Johnston et al.[15] first experimentally observed microwave oscillations and Nopoli and Ikola [16] reported stable reflection gain from a reverse biased Impatt-diode. Significant progress has been made in analytical techniques for the design of Impatt-oscillators and amplifiers and also their performance characteristics, in the subsequent decade. Parametric amplification and side band translation (frequency conversion) using negative resistance properties of Impatt devices were first reported in 1966 by Grace [1] and Clorfeine [2]. Since then, different analytical approaches and improvements have been suggested by various workers for detailed studies of the upconversion process in avalanche-diodes [3] - [7]. All the analysis techniques are based on Read's model and the i.f. signal level is considered to be weak compared with a strong "pump" or "carrier".

An approximate theory of two frequency interaction in the device is presented by Fakatsu [3]. Based on a simplified Read model of a diode with an abrupt junction and a triangular field pattern, impedance matrix coefficients are calculated in terms of the device parameters.

He also derived conditions for parametric negative resistance. Evans and Haddad [4], [5] presented a more extensive analysis for frequency-mixing properties of an oscillating diode by solving a nonlinear differential equation describing particle current in Impatt-diodes of relatively short transit time. A "self-pumped", two-port frequency converter was described in terms of its short circuit admittance parameters. In an extension of their work, Hines [7] derived parametric equations using an equivalent circuit for the Read diode model that included the effects of space charge and long transit times in the drift zone. Assuming linearisation of the relationship between ionization coefficients and the electric field, he reported important qualitative results for stability criteria for spurious oscillations of the "parametric" type, parametric amplification, frequency-conversion; noise-generation mechanism and noise enhancement by strong signals.

Shen et al. [6] studied, experimentally, the mixing properties of Impatt-diode by impressing an external signal with frequency close to the self-oscillating frequency of the oscillator. The beats could be experimentally observed and the device used as a down-converter. He also studied the optimisation of conversion gain with bias current and i.f. frequency. A net conversion gain using an Impatt-amplifier (47 GHz band) was reported by Kita and Kanmuri [9]. They studied the conversion characteristics, the bandwidth characteristics and pulsed behavior with 400 Mb/s PCM and the results were reported to be satisfactory for the upconverter to be used in millimeter-wave relay equipment. They suggested that the sum and difference frequency components are generated by parametric effects, when two frequency components are in-

jected into the device. Frequency components, close to the optimum frequency of the diode predicted by Read, get amplified because of the negative resistance of diode at those frequencies, thus resulting in conversion gain.

1.2 Outline of the Project:

Most of the analytical approaches for the study of frequency-conversion effects in Impatt-devices that have been reported, basically depend upon the Read model. Various simplifying assumptions have been incorporated in the models and some important conclusions and qualitative results have been reported. The Read model is recognized as an imperfect representation of real diodes; therefore, the results are only approximate for practical devices. Moreover, the analysis and results are presented in terms of physical parameters of the device, which though very important for understanding of the device and the process are often inconvenient for an engineer or designer to use.

The purpose of this project is to investigate another avenue of approach to analyse frequency conversion characteristics of avalanche diodes in terms of familiar engineering concepts. An analysis is presented based on admittance models of the device and the microwave circuit. This approach, in fact, is in line with Kita and Kanmuri's postulation on the conversion gain mechanism [9], mentioned in section 1.1.

The analysis, as presented, has its own limitations because of the many assumptions on which it is based.

The assumption that i.f. or signal level is quite weak as compared to a strong "pump" or microwave carrier, which has been the basis for almost all analysis on the topic in the past, is considered to hold for the present analysis as well. A further assumption is made, however,

that the weak bias signal does not affect the admittance versus frequency characteristics of the device. This assumption seems to hold upto a certain level of i.f. signal, as is evident from the results in Chapter IV. Any further assumptions made are explained during the course of discussion in the related chapters. The results presented are qualitative, although by extension of these concepts and a rigorous analysis it should be possible to obtain quantitative results.

A simple theory and some experimental results for Impatt-amplifiers are presented in Chapter II. Theoretical analysis and results for up-conversion in Impatt-amplifiers based on typical admittance characteristics are presented in Chapter III. In Chapter IV, experimental results obtained for two Impatt-amplifier upconverters are discussed and some of the characteristics are explained. An experimental investigation of distortion introduced by the amplifier upconverter, when the baseband (i.f.) signal is amplitude modulated, has been made. In the conclusion, Chapter V, the results of this research are summarized. Considerations for further research to enable better understanding of the upconversion phenomena in Impatt-diodes are outlined.

CHAPTER II

IMPATT-DIODE REFLECTION AMPLIFIERS

This chapter deals with the basic concepts involved in the anlaysis and design of Impatt-amplifiers. Several analytical techniques for the detailed study and design of avalanche-diode amplifiers are available in the literature. The admittance concepts that are relevant to the work in this thesis are discussed. Experimental results for two microwave Impatt-diode amplifiers, which were later used as upconverters, are presented.

2.1 Introduction

Considerable insight into the operation of the Impatt amplifier has been obtained since the time that it was first used as a stable gain reflection amplifier by Napoli and Ikola [16]. The admittance characteristics of the device and the circuit have been recognised as convenient tools for the understanding, as well as for analysis, of Impatt-amplifiers. The charge equations of the Read model have been solved for the study of small and large signal admittance behavior of the device [20], [21] and accurate methods are presently available for the measurement of these characteristics [22], [23], [24]. Many important amplifier characteristics such as gain, phase, bandwidth etc., can be predicted [12] from the real admittance data. The analysis of Impatt-amplifier characteristics, based on typical admittance data, is discussed in the following sections. It should be noted that the device admittance for the actual Impatt diodes used for the measured results, will be different from the data for the "typical" device. However, it is expected that the device admittance behavior will be similar, so that the predicted theoretical results and the measured results will be qualitatively comparable.

2.2 Admittance Characteristics of an Impatt-amplifier:

The device and circuit or load admittances measured by Laton and Haddad [12] for a typical amplifier are shown in Figure 2.1. These plots are referred to as a Device-Circuit diagram. The measurements were made for a silicon Read device with an assumed area of $10^{-4}cm^2$, 4μm length and a 1μm avalanche region width. The diode was mounted in a 50 Ω coaxial cavity with a 32Ω quarter wavelength slug tuning. The bias current density was $500A/cm^2$ and the reference plane for admittances was taken as the chip itself, using the equivalent circuit as determined by Greiling and Haddad [20].

The following general observations about the admittance characteristics of an Impatt-diode can be made from the plots in Figure 2.1.

The negative conductance of the device varies significantly with frequency over the useful range of operation. The implication of this feature is that wide band performance of the device is severely degraded and special considerations have to be given in broadband design.

Both real and imaginary parts of the device admittance are strongly dependent on r.f. signal level. The rapid increase in the device susceptance with r.f. voltage occurs because an increase in r.f. voltage causes an increase in the conduction current. This, in turn, causes a nonlinear increase in the space charge in the diode during the generation of carriers. Thus, the capacitive susceptance of the device increases nonlinearly with increase in r.f. signal. Also, due to an increase in the space charge, the field in the avalanche region is flattened over a wider region. Thus the carriers are generated over a broader region and transit angle of the carriers is spread over a wider range. Only a few

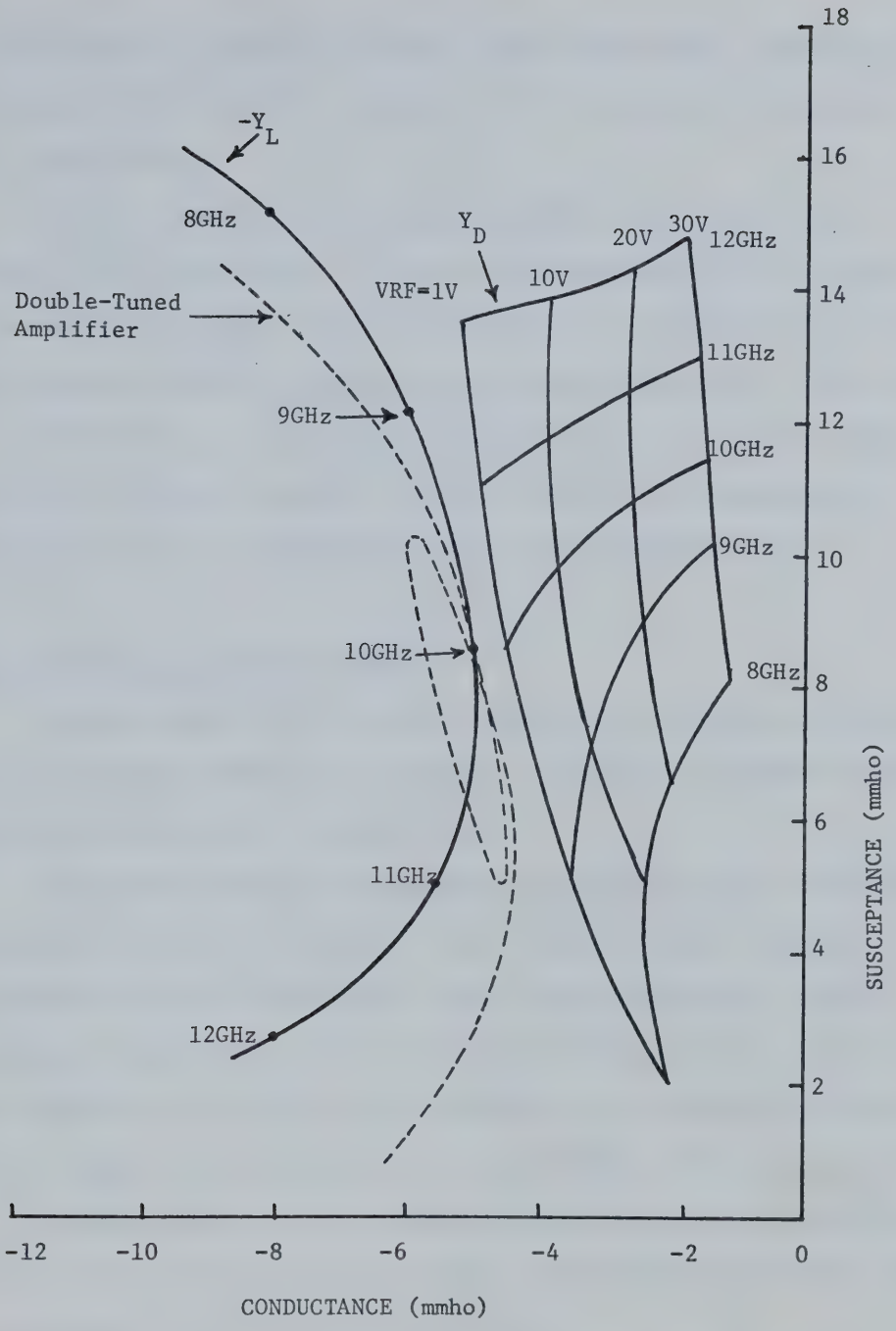

FIG. 2.1 DEVICE-CIRCUIT DIAGRAM FOR A TYPICAL IMPATT-DIODE AMPLIFIER

of the carriers experience the same optimum phase delay, thus causing a decrease in the negative conductance of the device with increase in r.f. signal level.

The diode admittance also depends strongly upon the d.c. bias current through the device. A study of the admittance variation with bias current shows that negative conductance increases with increasing bias current, while the susceptance decreases only slightly [20], [23].

The dependence of admittance characteristics on different doping profiles, different materials such as Si, Ge and GaAs, has been investigated in the literature but will not be discussed here.

2.3 A Reflection Amplifier Model:

A model, described by Laton and Haddad [12] and useful in predicting the nonlinear behavior of reflection amplifiers, employing discrete device admittance data is discussed here.

A schematic diagram of a circulator coupled reflection type Impatt-amplifier is shown in Figure 2.2. The reference plane for analysis is considered to be the diode wafer itself, the diode package, cavity, tuning and transforming network impedance being part of the circuit or load impedance. The circulator is assumed to be broad-band and ideal, and the source as well as the load are considered to be perfectly matched.

The power gain of a reflection-type negative resistance amplifier is given by the square of its reflection coefficient and the phase shift by the angle of the reflection coefficient:

$$\text{Power Gain } P = |\Gamma|^2 = \left| \frac{Y_L - Y_D^*}{Y_L + Y_D} \right|^2 \qquad (2.1)$$

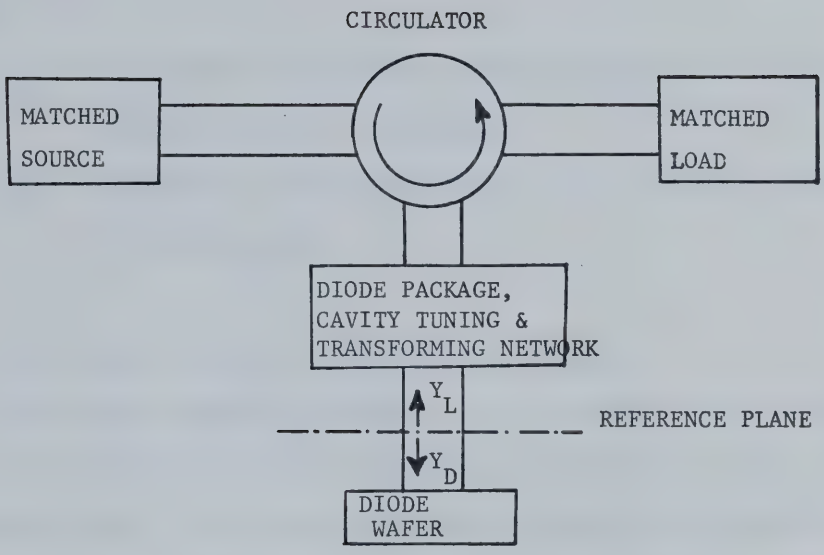

FIG. 2.2 A SCHEMATIC DIAGRAM OF REFLECTION TYPE AMPLIFIER

$$\text{Phase } \phi = \angle\Gamma = \tan^{-1}\left[\frac{\Gamma - \Gamma^*}{\Gamma + \Gamma^*}\right] \qquad (2.2)$$

where

Y_D = Admittance seen looking towards the device at a convenient reference plane (diode wafer).

Y_L = Admittance seen looking away from the device at the same reference plane.

The asterisk indicates the complex conjugate.

For single frequency operation, the expressions (2.1) and (2.2) can be used to calculate the theoretical gain and phase shift at the reference plane. It is implicitly assumed that all the harmonics of the r.f. voltage are shorted by the diode package and the microwave circuit.

Representing admittances as vectors in the complex admittance plane, the numerator and denominator of (2.1) can also be represented as vectors $\vec{N}$ and $\vec{D}$ respectively as shown in Figure 2.3.

In terms of $\vec{N}$ and $\vec{D}$, therefore,

$$\text{Power Gain } P = \frac{|\vec{N}|^2}{|\vec{D}|^2} \qquad (2.3)$$

where

$$\text{Numerator vector } \vec{N} = \vec{Y}_L - \vec{Y}_D^* \qquad (2.4)$$

$$\text{Denominator vector } \vec{D} = \vec{Y}_D + \vec{Y}_L = \vec{Y}_D - (-\vec{Y}_L) \qquad (2.5)$$

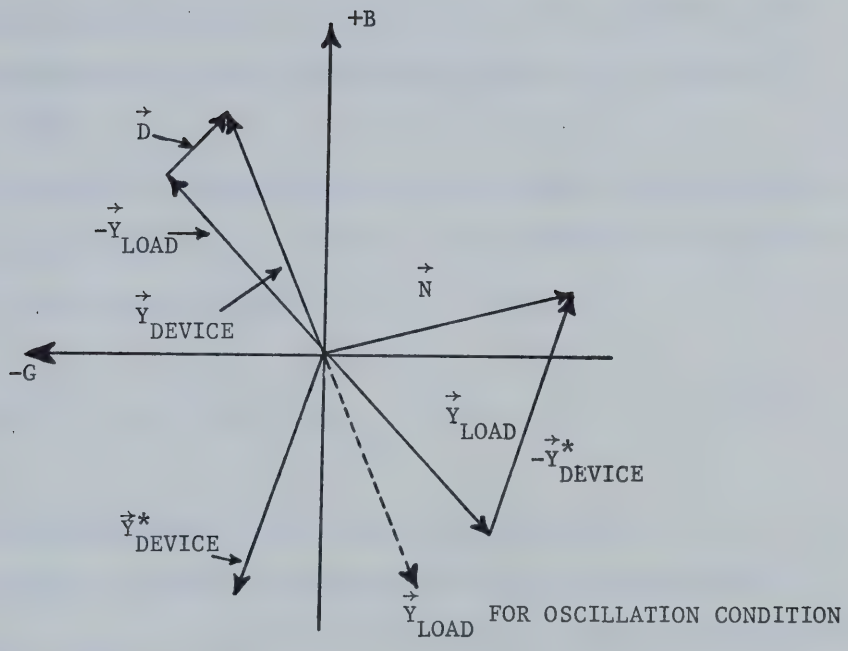

Fig. 2.3 COMPLEX PLANE REPRESENTATION OF DEVICE AND CIRCUIT ADMITTANCE

For a large negative conductance, $\vec{Y}_D$ can be comparable to $-\vec{Y}_L$ so that $\vec{D}$ is much smaller than $\vec{N}$. This gives a large power gain. Also, any small change in load or device admittance will cause a relatively large change in $|\vec{D}|$ and an insignificant change in $|\vec{N}|$. For high gains, therefore, the performance characteristics of Impatt-amplifiers can be studied by examining $1/|\vec{D}|$.

In the limit as $|\vec{D}|$ approaches zero, power gain becomes infinite and oscillations will occur. From (2.4) the condition of oscillation in terms of admittances, becomes:

$$|\vec{D}| = 0 \quad \text{or} \quad \vec{Y}_L = -\vec{Y}_D \tag{2.6}$$

which is indicated on the vector diagram in Figure 2.3.

Considering the device admittance to be in the second quadrant away from the origin (large capacitive susceptance and negative resistance of the device), then using Figure 2.1, the characteristics of the amplifier can be explained as follows:

1. Since the device and load admittance curves do not intersect, the amplifier is stable. An implied stability requirement therefore becomes that the real part of circuit admittance must be larger than the magnitude of the real part of the device admittance.
2. Approximate magnitude of the gain will be inversely proportional to the distance between negative of circuit and device operating points. Maximum gain is expected near a frequency of 10 GHz where $|\vec{D}|$ is minimum.

3. As the level of the microwave signal increases, $|\vec{D}|$ increases but undergoes a smaller percentage variation with frequency. Therefore, reduced peak gains with large bandwidths may be expected.
4. As discussed in the previous section, the device susceptance is an increasing function of r.f. voltage. As the input power level increases, the frequency at which peak gain occurs should, therefore, shift downwards. For the same reason, the frequency at which phase shift in the amplifier is zero should shift downwards with increasing input power levels.

Theoretical calculations of Impatt-amplifier gain, from typical admittance data in Figure 2.1, as a function of frequency were made (Figure 2.4). All the observations made in the above discussion are quite apparent from these plots.

For a broadband reflection gain amplifier the requirement can be explicitly defined in terms of the circuit admittance behavior for a given device. It is required that the (negative) circuit admittance should run parallel to the device admittance curve with its real part always greater than that of the device and with its imaginary parts being equal at all frequencies within the operating range. An exact realization of such a requirement seems to be very difficult because the circuit susceptance behaviour displays frequency dependence opposite to that defined above, as evident from Figure 2.1. However, using a somewhat complicated tuning scheme it is possible to meet the above requirement over a limited frequency range. This happens when a loop can be formed in the circuit admittance characteristics using additional tuning elements. The requirement is indicated by dotted circuit admittance curve in Figure 2.1. More care is needed in tuning while using such a scheme,

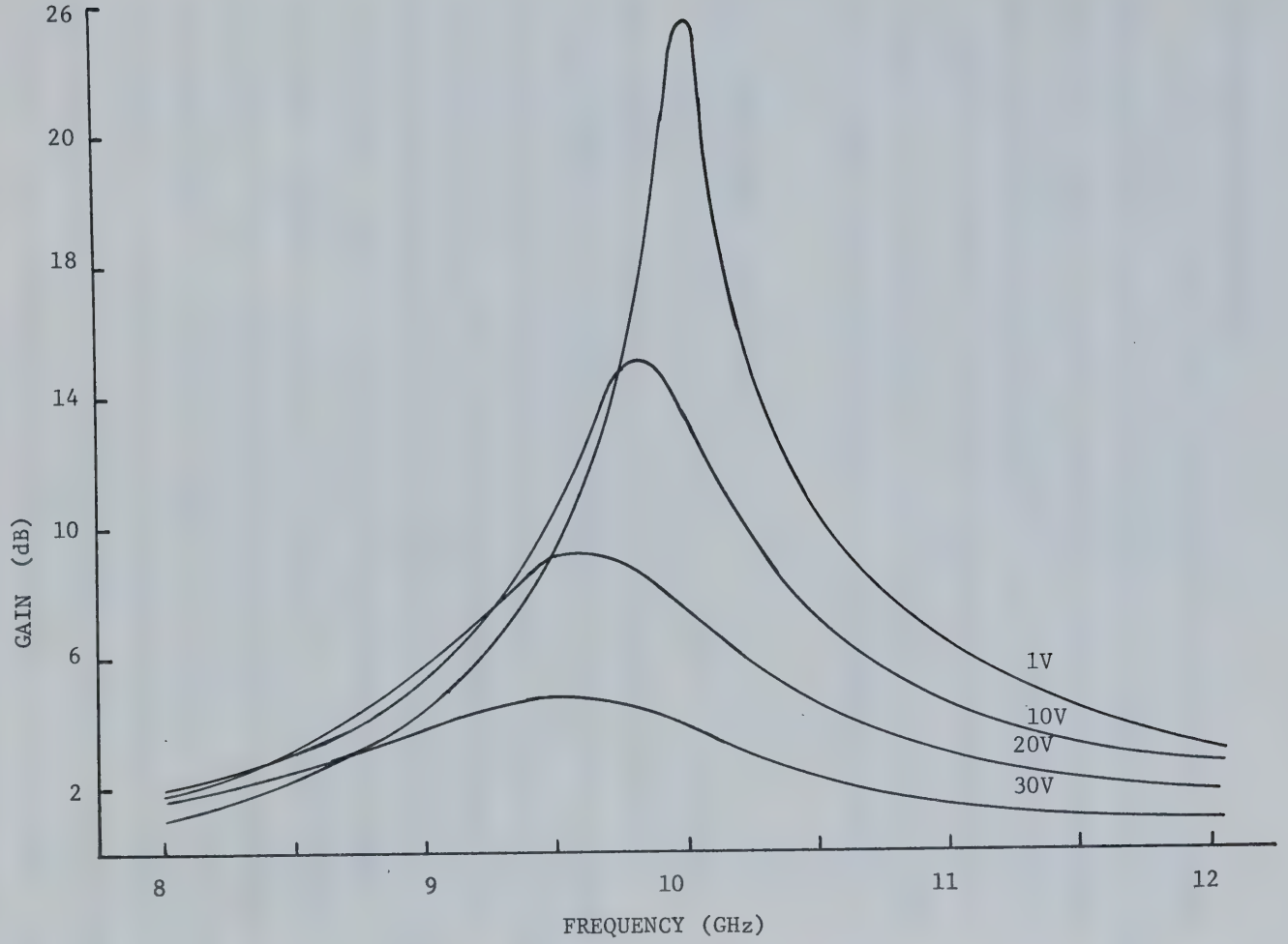

FIG. 2.4 THEORETICAL AMPLIFIER GAIN VS. FREQUENCY CHARACTERISTICS OF THE IMPATT-AMPLIFIER FROM TYPICAL ADMITTANCE DATA

because the amplifier tends to be unstable for many tuning positions.

2.4 Experimental Results:

Experimental results were obtained for two amplifiers; a single-tuned narrow band coaxial cavity amplifier and a double-tuned relatively broad band waveguide amplifier. The device used for both the set ups was an HP5082-0435 X-band Impatt-diode. Since the analysis is done in a qualitative sense only, the results presented are measured at the output port of the amplifier. The measurements were made on a point by point basis using the experimental set up discussed in section 2.4.1.

2.4.1 Measurement Circuit Used:

The circuit used for measurement of the amplifier performance characteristics is shown in Figure 2.5. A three-port circulator (Sperry D43X21) with a minimum isolation of 20 dB was used to separate the output of the reflection amplifier from the input. The input and output were sampled by using two 10 dB (HPX752C) directional couplers. By means of waveguide switches the input frequency and power level as well as the output spectrum and power level were monitored. The sweep oscillator (HP8620A) was operated in CW mode for all the measurements except when the amplifier gain characteristics were to be observed on the oscilloscope. In the swept frequency measurements the sweep output was applied to the horizontal input of the oscilloscope and the d.c. output from the detector mount went to the vertical input. The gain versus frequency characteristics could be displayed on the scope screen. Two precision attenuators (HP/-X382A) were used in the input and output. A slide-screw tuner is normally required for the tuning of amplifiers.

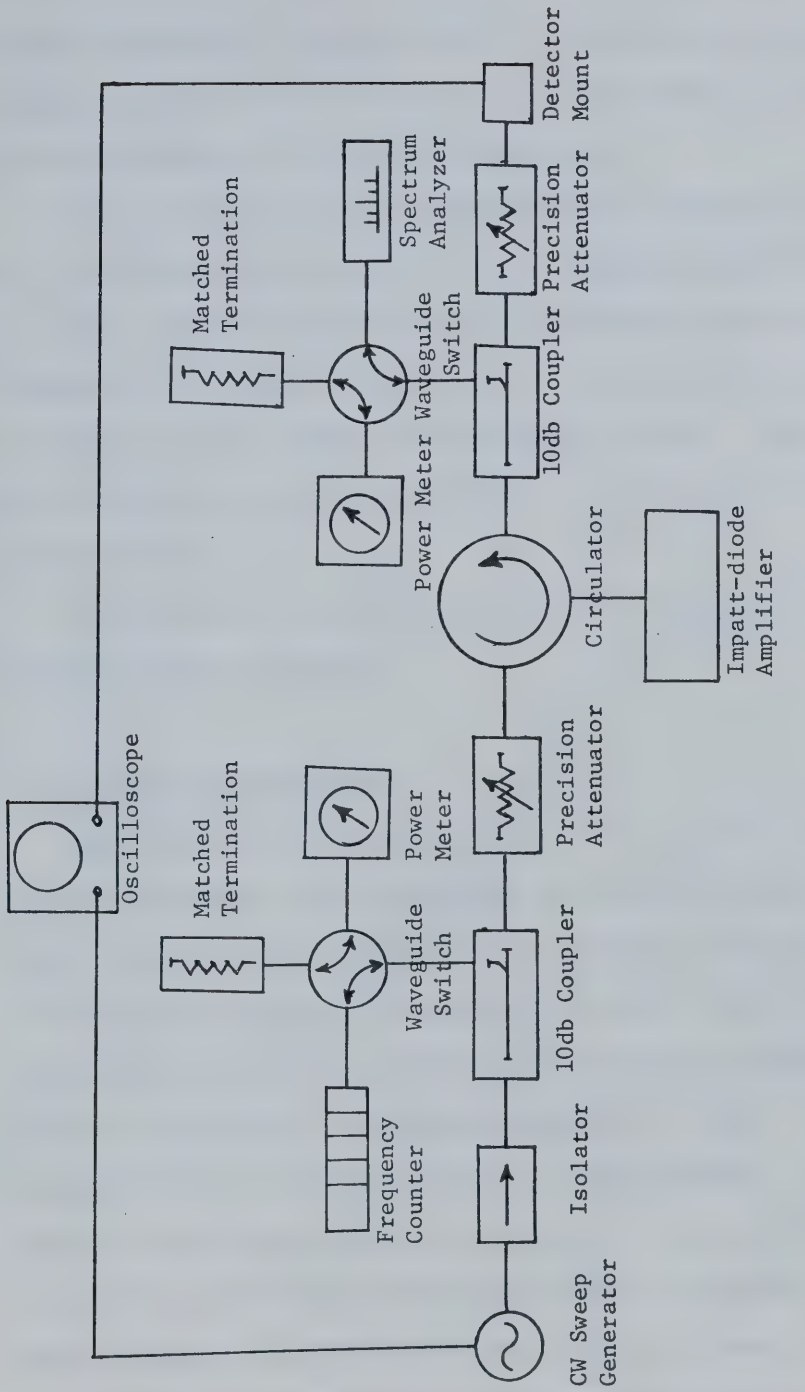

FIG. 2.5 CIRCUIT DIAGRAM FOR MEASUREMENT OF IMPATT-AMPLIFIER CHARACTERISTICS

Careful adjustment of the tuner could be done while observing the output spectrum on the spectrum analyzer (HP-8555A; r.f. section) and the gain response on the oscilloscope screen.

Phase shift introduced by amplifiers was measured by using a magic-tee. Input signal was applied at port 1 through a phase shifter and the output signal was applied to port 2 through an attenuator, port 4 being match terminated. Phase at port 1 and attenuation at port 2 could be adjusted to get a power null (minimum) at port 3. The circuit could first be characterised by putting a short at the amplifier port of the circulator.

The device was protected from power line transients by a SCR triggered crow-bar circuit.

2.4.2 Single-tuned Amplifier:

Experimental observations were made for a d.c. bias current of 29.5 mA and using a slide-screw tuner as the tuning element. Gain versus frequency characteristics of the amplifier are shown in Figure 2.6. Small signal gain at -20dBm (0.01 milliwatt) input is 15 d with a 3 db bandwidth of 10MHz. At 0dBm (1 MW) input, the amplifier gain drops down to 4 dB and the 3 dB bandwidth increases to 38MHz. The shift in frequency at which peak gain occurs is clearly evident. Figure 2.7 presents input-output power characteristics of the amplifier. Saturation of the device occurs when large input signals are applied. Phase shift versus frequency for four input power levels is plotted in Figure 2.8. It is seen that the frequency at which the phase shift introduced by the amplifier is zero shifts downwards as the input power level is increased.

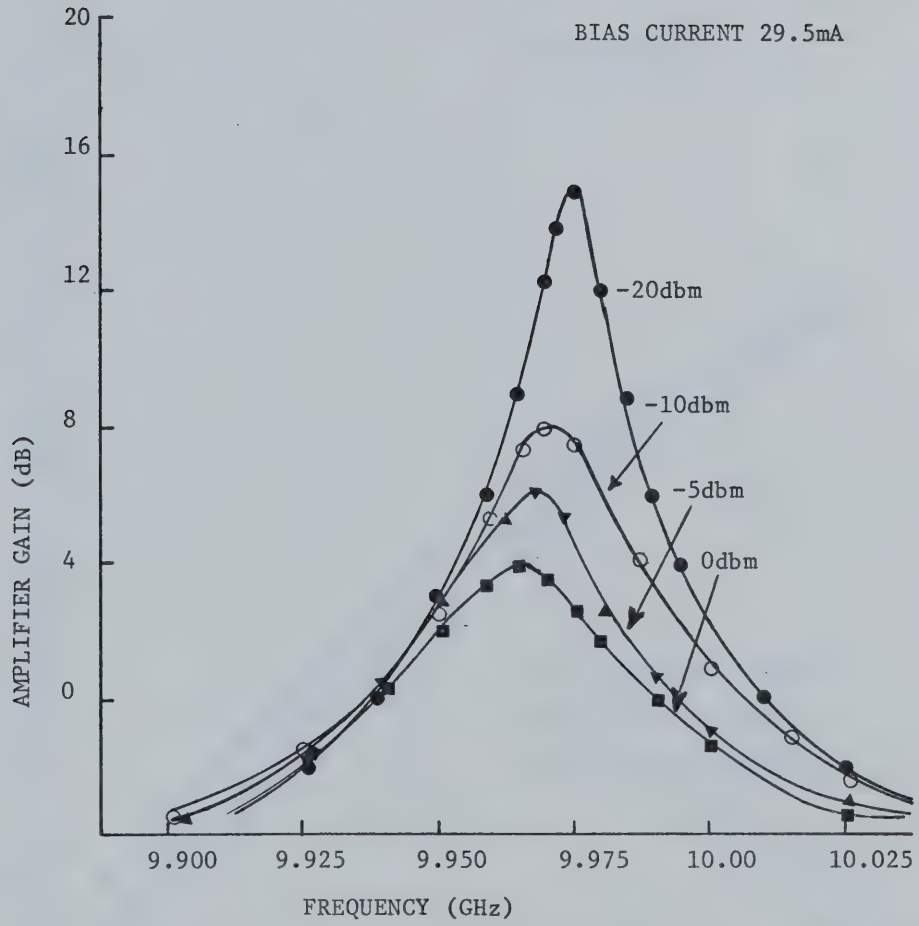

FIG. 2.6 GAIN VS. FREQUENCY CHARACTERISTICS OF SINGLE TUNED AMPLIFIER

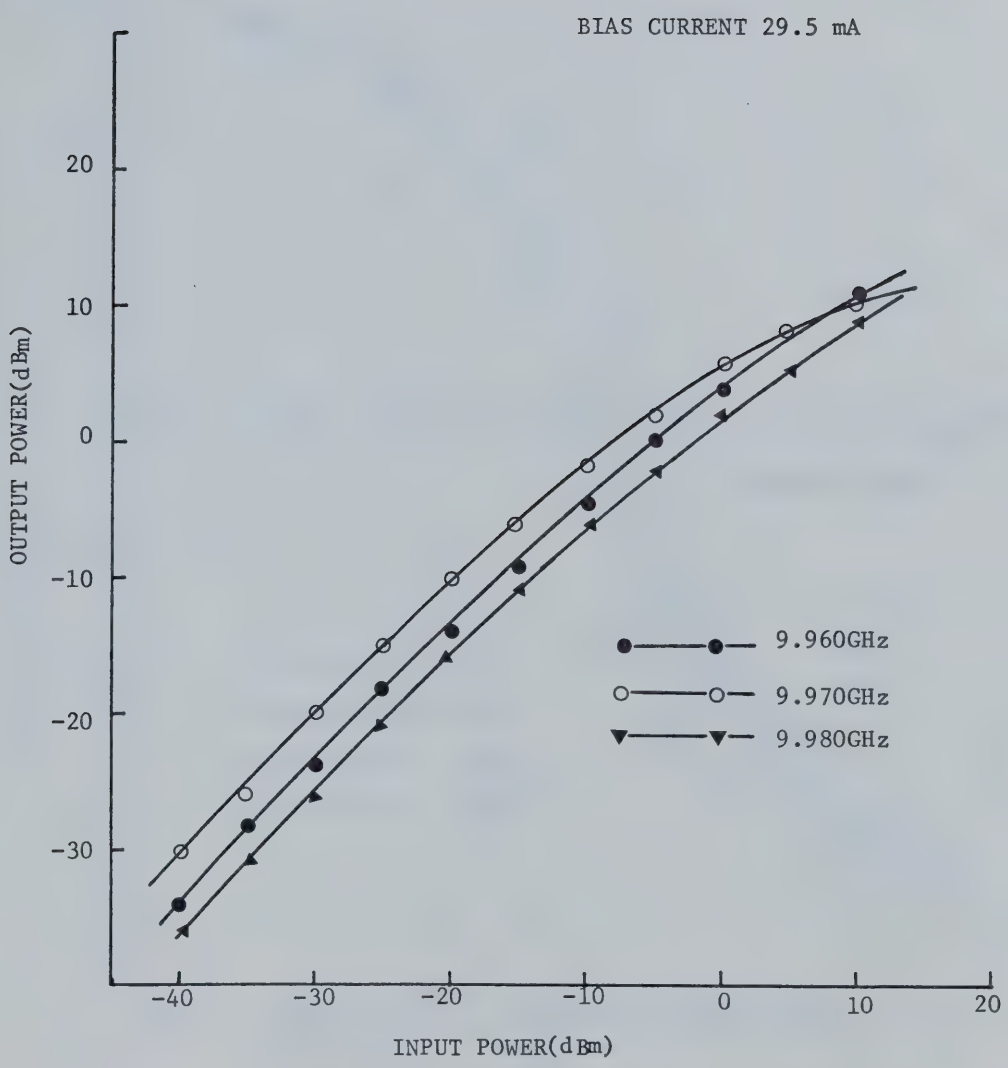

FIG. 2.7 OUTPUT VS. INPUT POWER FOR SINGLE TUNED AMPLIFIER

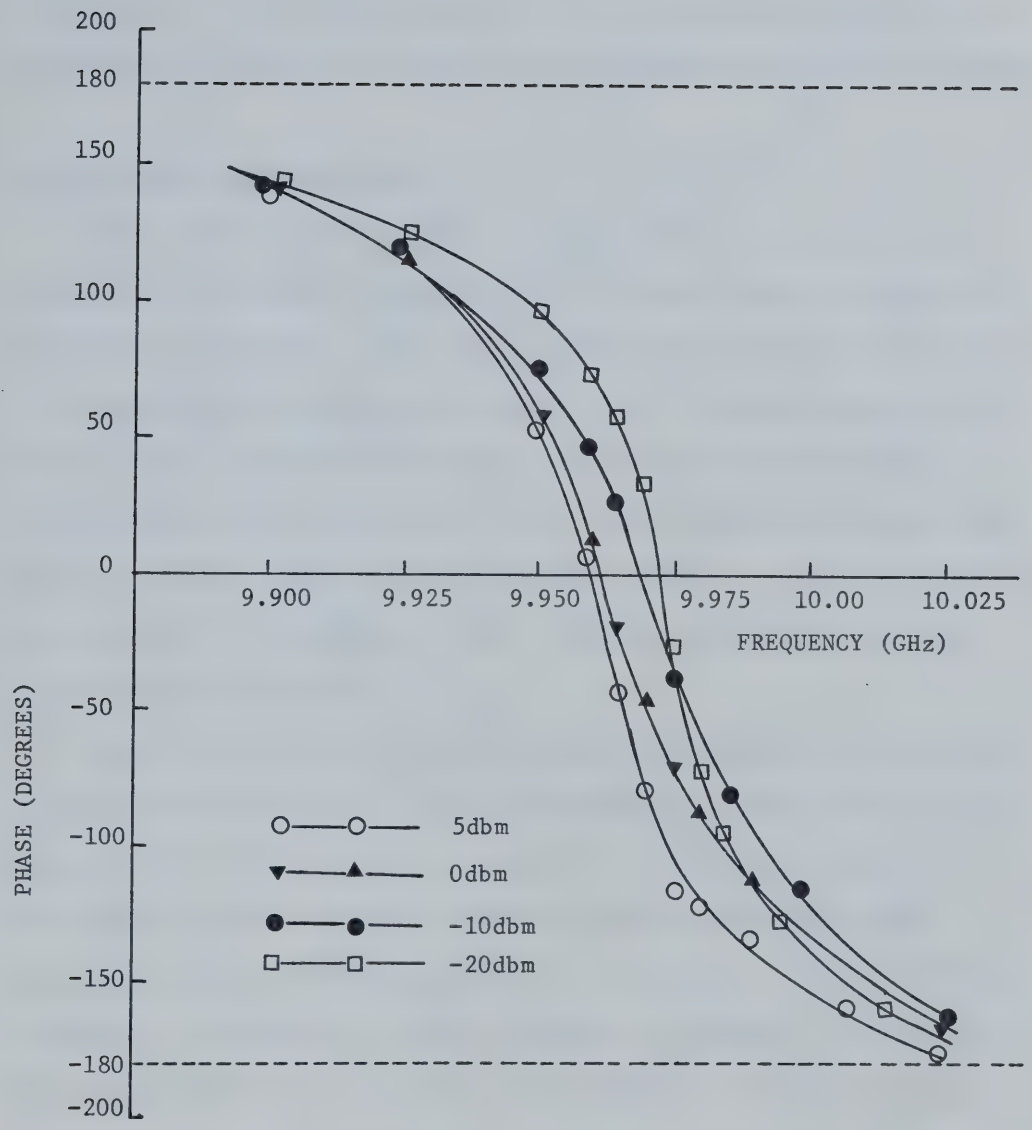

FIG. 2.8 PHASE SHIFT VS. FREQUENCY CHARACTERISTICS OF THE SINGLE TUNED AMPLIFIER

The results obtained for the amplifier are in good qualitative agreement with the expected amplifier characteristics discussed in section 2.3. This suggests that the circuit admittance curve for the amplifier was smooth as in Figure 2.1, but changes rapidly with frequency.

2.4.2 Double-tuned Amplifier:

Two tuning elements, an E-H tuner and a slide screw tuner, were used for this waveguide amplifier. The d.c. bias current through the device was maintained at 30mA. Gain versus frequency characteristics of the amplifier are presented in Figure 2.9. A small-signal peak gain of 21db with a 3db bandwidth of 40MHz and 1db bandwidth of 13MHz is available with -30dbm input power level. For -10dbm input power, peak gain is reduced to 16db and the bandwidth increases to 60MHz within 1.5db gain variation. Gain peaks at lower frequency (10GHz) for 0dbm and higher input power levels.

Figure 2.10 presents information about saturation of the amplifier at different frequencies. The gain expansion for lower frequencies at higher power levels is evident. It may be of particular interest to note that input power levels at which departure from small-signal operation occurs is highly dependent on the frequency. Phase-shift introduced by the amplifier versus frequency at different power levels is plotted in Figure 2.11. The phase shift within the frequency range of interest is 360°. The double-peak in the gain plots suggests the existence of a loop in the circuit admittance characteristics of the amplifier.

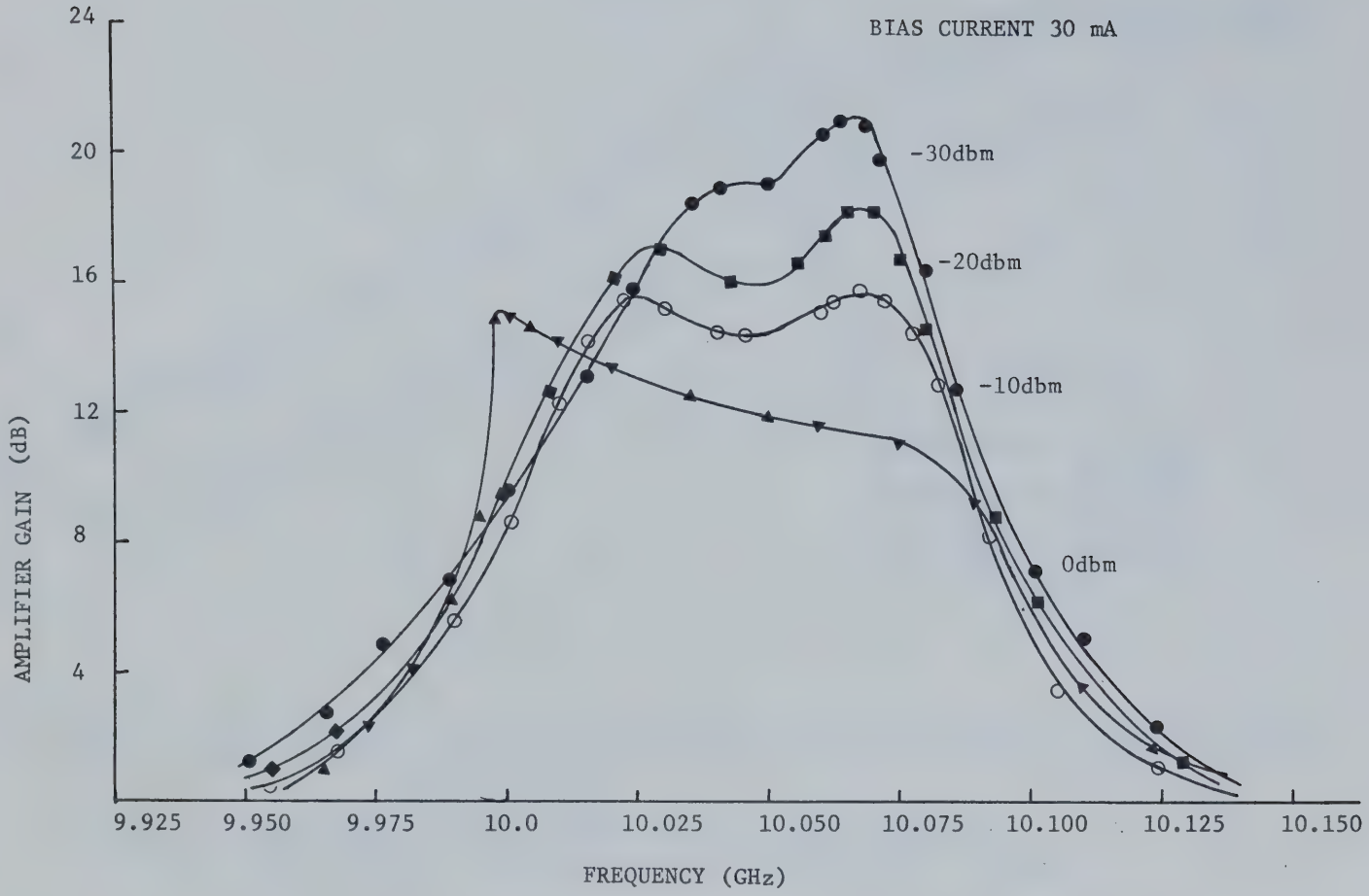

FIG. 2.9 GAIN VS. FREQUENCY CHARACTERISTICS OF DOUBLE TUNED AMPLIFIER

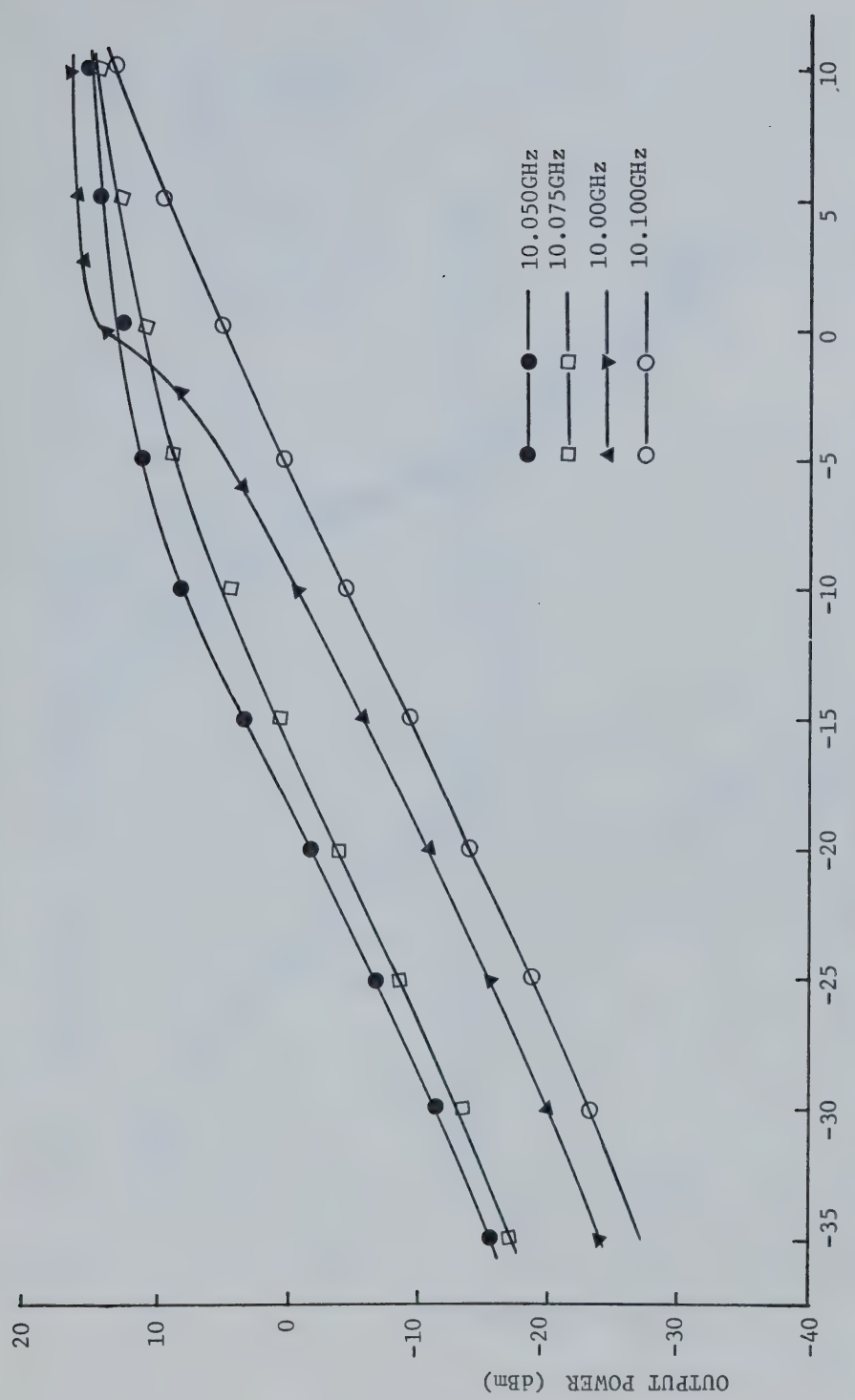

FIG. 2.10 OUTPUT POWER VS. INPUT POWER FOR DOUBLE TUNED AMPLIFIER

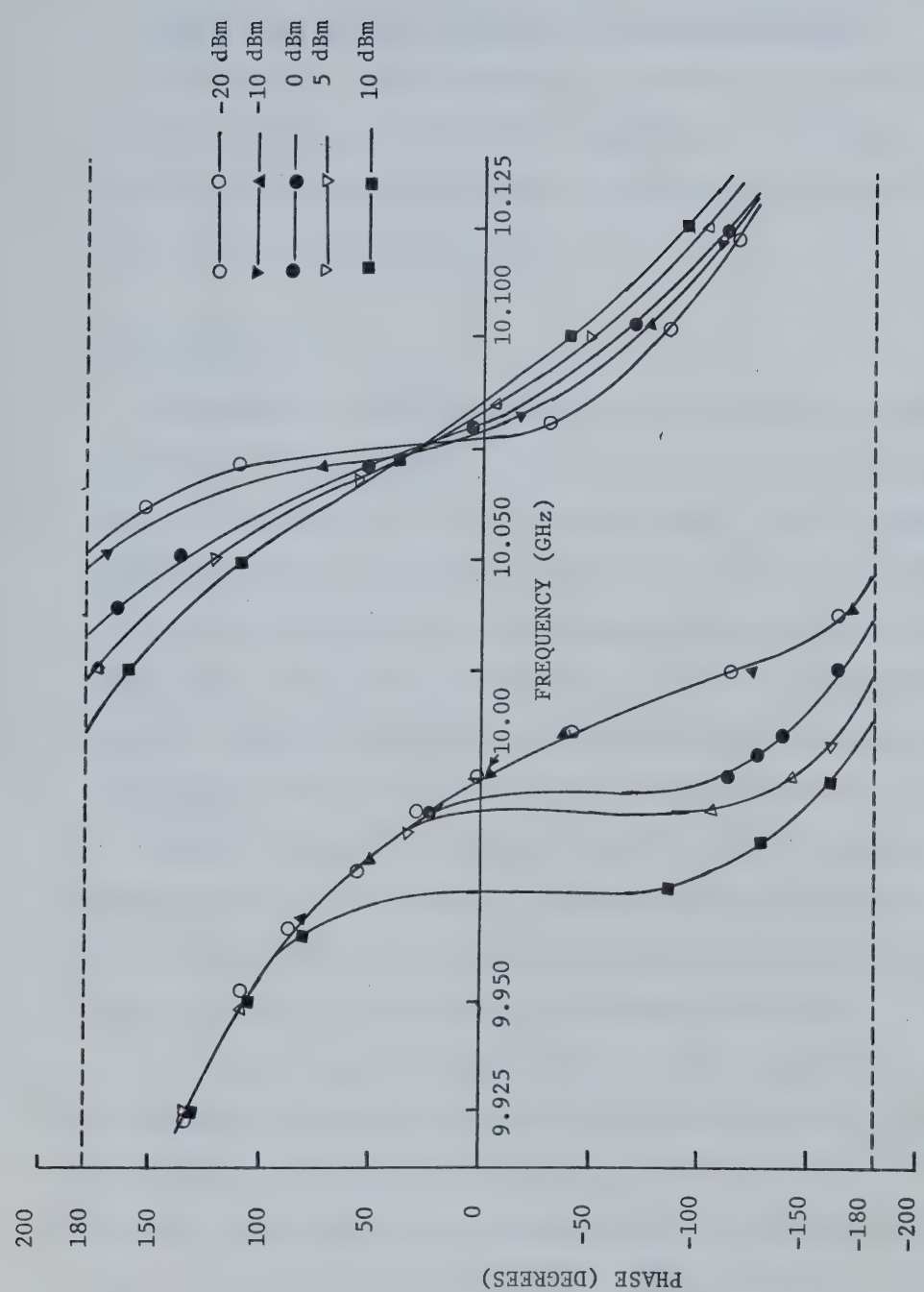

FIG. 2.11 PHASE SHIFT VS. FREQUENCY PLOT FOR THE DOUBLE-TUNED AMPLIFIER

CHAPTER III

THEORETICAL ANALYSIS OF IMPATT AMPLIFIER UPCONVERTERS

A simple small signal analysis for the investigation of upconversion characteristics of Impatt-amplifiers is discussed. Theoretical results from admittance considerations are calculated by use of simple computer programmes.

3.1 Introduction:

Upconversion in Impatt-amplifiers may be achieved by impressing the base-band (i.f.) signal on the bias circuit, while a microwave signal is applied to the input of the amplifier. The i.f. signal causes bias current modulation of the device, and because of non-linearity of the avalanche process, mixing of the two applied frequencies takes place so that sum and difference frequencies are generated. Because of the band-limiting property of the amplifier and negative resistance of the device, some of the frequency components are amplified. The upconverted signal at microwave frequency can be separated out by making use of suitable filters. Another method of achieving upconversion with an Impatt-device is to modulate the bias current of an oscillating diode and then filter out one of the sidebands generated.

Apart from some experimental work [7] - [10], most of the theoretical work on this topic has been done using the Read model [1] - [6]. In many cases, the analysis is applicable to oscillators only [1] - [4]. The results discussed are qualitative and hold for practical devices only to the extent that the Read model represents practical diodes. An alternate method for the study of upconversion characteristics of

Impatt-amplifiers, based on the admittance behavior of the device and the circuit, will be the subject matter of the following sections.

3.2 Small-signal Model:

For the purpose of analysis, the problem of upconversion reduces to that of two (or more) frequencies interacting in a highly nonlinear device embedded in a microwave circuit. The non-linearity of the device strongly depends upon the frequency and power level of the input signal, the d.c. bias current and possibly the impressed i.f. signal. An exact study of such a problem is difficult, if not impossible, and for an accurate analysis a lot of computer time might be consumed in characterising each non-linearity separately.

With some assumptions and within certain limitations, however, a simple and approximate small signal theory may be used that explains the phenomena reasonably well. The analysis is based on the following assumptions:

a. The i.f. signal is sufficiently weak as compared to a strong microwave or "pump" signal,

b. The weak i.f. signal does not affect the admittance versus frequency characteristics of the device, and

c. The intermediate frequency is low enough, so that the circuit and device admittances do not change significantly over the frequency band of centre frequency and side bands.

The last assumption is perhaps the biggest limitation of this analysis. Nonetheless, the analysis is important for understanding the conversion process and for providing a basis for further extensions and improvements.

The small signal model, which is an extension of the admittance model explained in the previous chapter, is shown in Figure 3.2. Bias current modulation due to the low frequency base-band signal, can be considered to cause variations in device admittance vector at the signal frequency. These admittance vector variations cause a relatively larger percentage variation in the denominator vector $\vec{D}$ as compared to numerator vector $\vec{N}$. The reflection coefficient of a negative resistance amplifier is given by:

$$\Gamma = \frac{Y_L - Y_D^*}{Y_L + Y_D} = \frac{N}{D} \qquad (3.1)$$

where N and D are complex quantities.

For an applied i.f. signal that bias modulates the amplifier, time dependent $\tilde{\Gamma}$ will become:

$$\tilde{\Gamma} = \frac{Y_L - Y_D^* - \tilde{Y}_d^*}{Y_L + Y_D + \tilde{Y}_d} \qquad (3.2)$$

Where Y_L is the complex load or circuit admittance as seen from the reference plane (device wafer),

Y_D is the complex device admittance when no external bias signal is applied, and

$\tilde{Y}_d$ is the variation in the admittance vector dependent upon the applied i.f. voltage.

The admittance variations for any applied bias current modulation at frequency ω_1 can be represented as:

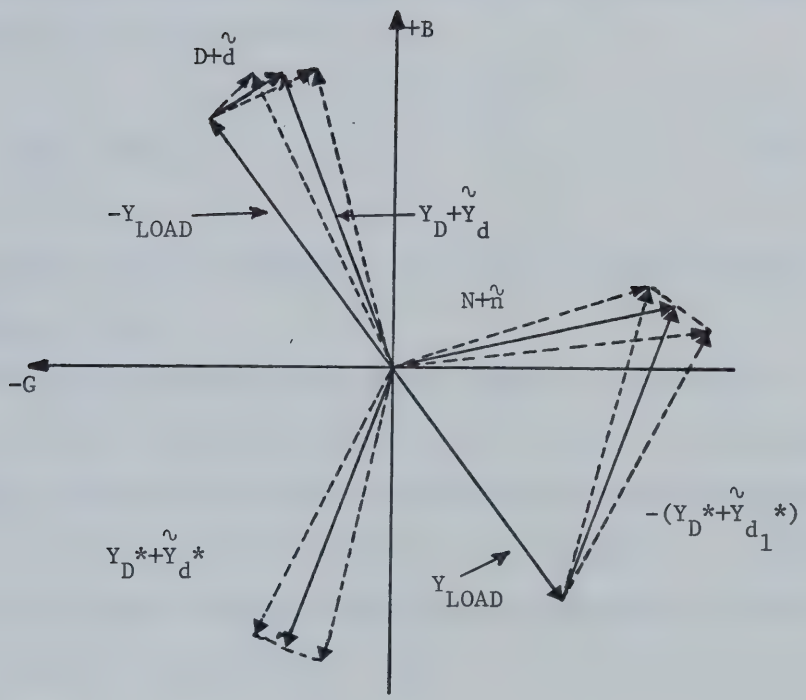

FIG. 3.1 ADMITTANCE MODEL FOR BIAS MODULATED IMPATT-AMPLIFIERS

$$\tilde{Y}_d = \sum_{n=o}^{\infty} |Y_{d_n}| \, e^{jn\omega_1 t} \tag{3.3}$$

where $|Y_{d_n}|$ is the magnitude of admittance variation component at nth harmonic. Of prime important however, is the first order variation of $\tilde{Y}_d$ for weak i.f. signals. This in a sinusoidal representation can be written as:

$$\tilde{Y}_d = |Y_{d_1}| \, \text{Sin}\omega_1 t \tag{3.4}$$

For small signals at fixed ω_1, $|Y_{d_1}|$ will be linearly related to i.f. voltage, $V_{i.f.}$.

During investigations of admittance behavior with change in current density, it has been reported [19], [22] that with an increase in the bias current the negative conductance of the device increases whereas its susceptance varies only slightly. Therefore, to simplify the analysis further, the small variations of susceptance, if any, due to bias signal are neglected, that is:

$$\tilde{Y}_{d_1} \tilde{=} [-G_{d_1} + jo) \, \text{Sin}\omega_1 t \tag{3.5}$$

Substituting (3.5) for $\tilde{Y}_{d_1}$ in (3.2) we get:

$$\tilde{\Gamma} = \frac{N + Y_{d_1} \, \text{Sin}\omega_1 t}{D - Y_{d_1} \, \text{Sin}\omega_1 t} \tag{3.6}$$

$$= \frac{N/D + Y_{d_1}/D \, \text{Sin}\omega_1 t}{1 - Y_{d_1}/D \, \text{Sin}\omega_1 t} \tag{3.7}$$

For $\tilde{\Gamma}$ to be finite at all times, Y_{d_1}/D should be less than unity, which defines the condition of stability for the amplifier upconverters.

Expanding Equation (3.7) into a power series:

$$\tilde{\Gamma} = [N/D + \frac{Y_{d_1}}{D} \mathrm{Sin}\omega_1 t][1 + \sum_{n=1}^{\infty} (\frac{Y_{d_1}}{D})^n \mathrm{Sin}^n\omega_1 t \qquad (3.8)$$

$$= N/D + (1 + N/D) \sum_{n=1}^{\infty} (\frac{Y_{d_1}}{D})^n \mathrm{Sin}^n\omega_1 t \qquad (3.9)$$

Substituting in (3.9):

$$\Gamma = N/D \qquad (3.10)$$

and

$$\beta = Y_{d_1}/D \qquad (3.11)$$

both Γ, β being complex quantities; we get:

$$\tilde{\Gamma} = \Gamma + [1 + \Gamma] \sum_{n=1}^{\infty} \beta^n \mathrm{Sin}^n\omega_1 t \qquad (3.12)$$

where $\beta < 1$ for stable upconverters.

$\mathrm{Sin}^n\omega_1 t$ terms can be expanded into constant, $\mathrm{Sin}\omega_1 t$, $\mathrm{Sin}2\omega_1 t$, ..., $\mathrm{Sin}n\omega_1 t$ terms.

Each even value of n in (3.12) makes contribution to the constant component of Γ and even harmonic terms of ω_1 and each odd value contributes towards $\mathrm{sin}\omega_1 t$ and odd harmonic terms. The expansion can be expressed as:

$$\tilde{\Gamma} = [\Gamma + [1 + \Gamma][1/2\ \beta^2 + 3/8\ \beta^4 + 5/16\ \beta^6 + \ldots + [\frac{^{K}C_{K/2}}{2^K}]\ \beta^K + \ldots]_{K \text{ even}}]$$

$$+ \text{Sin}\omega_1 t[1 + \Gamma][3/4\ \beta^3 + 5/8\ \beta^5 + 35/64\ \beta^7 + \ldots + [\frac{^{K}C_{K-1}}{2^{K-1}}]\ \beta^K + \ldots]_{K \text{ odd}}$$

$$+ \text{Cos}2\omega_1 t[1 + \Gamma][\beta^2[1 + \Gamma] + \ldots\ldots] + \ldots\ldots \qquad (3.13)$$

The coefficients $[C^K_{K/2}/2^K]_{K \text{ even}}$ and $[\frac{^{K}C_{K-1}}{2^{K-1}}]_{K \text{ odd}}$ are both monotonically decreasing functions of K. Their values up to K=30 are given in Table 3.1. Also since β is always less than unity, the infinite series in coefficients of the constant and $\text{Sin}\omega_1 t$, $\text{Sin}2\omega_1 t$ ... terms are convergent.

At the output port we will get

$$V_{out} = \tilde{\Gamma}|V_{in}|\ \text{Sin}\omega_p t \qquad (3.14)$$

ω_p being the microwave "pump" frequency.

Equation (3.14) gives all the frequency components present in the output. The output spectrum therefore should be as shown in Figure 3.2. The first order components, one below and the other above the centre frequency are the largest and of prime importance. Further analysis in this work, mainly concentrates on these sidebands and the centre frequency component.

The time independent term directly gives the voltage gain at the centre or microwave frequency while the $\text{Sin}\omega_1 t$ term will give rise to

Table 3.1 Coefficients of the Power Series Terms in Equation (3.13)

K odd		K even	
K	$C^K_{K-1/2}$	K	$C^K_{K/2}/2^K$
1	1.0	2	0.5
3	0.75	4	0.375
5	0.625	6	0.312
7	0.547	8	0.273
9	0.492	10	0.246
11	0.451	12	0.226
13	0.419	14	0.209
15	0.393	16	0.196
17	0.371	18	0.185
19	0.352	20	0.176
21	0.336	22	0.168
23	0.322	24	0.161
25	0.310	26	0.155
27	0.299	28	0.149
29	0.289	30	0.144

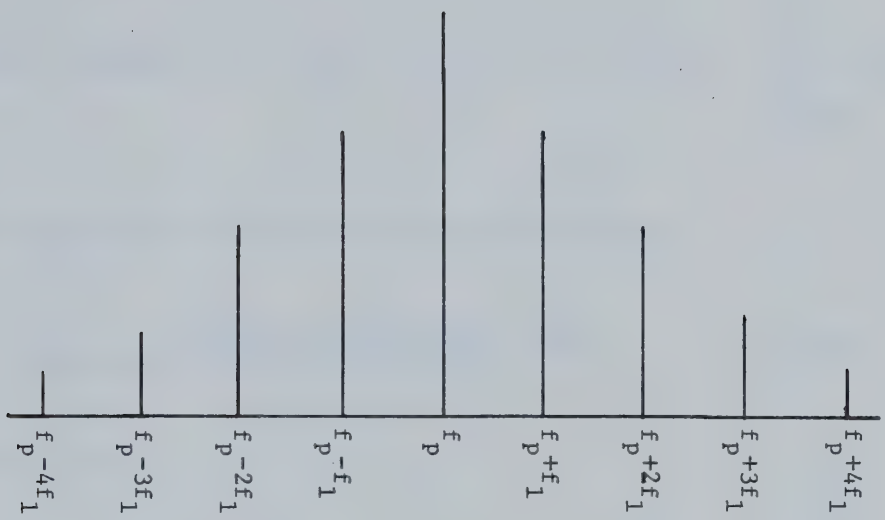

f_p = Input "pump" or microwave frequency

f_1 = Bias modulation or intermediate frequency

FIG. 3.2 OUTPUT SPECTRUM OF THE AMPLIFIER UPCONVERTER

two equal sideband components.

From equations (3.13) and (3.14), the centre frequency gain will be given by:

$$\text{CF Gain} = 20 \log \Gamma + [1 + \Gamma][1/2\ \beta^2 + 3/8\ \beta^4 + 5/6\ \beta^6 + \ldots + \frac{{}^{K}C_{K/2}}{2^K}\ \beta^K + \ldots]_{k \text{ even}} \tag{3.15}$$

and the microwave conversion efficiency, defined as:

$$\eta_{\text{conversion}} = \frac{\text{Upconverted (sideband) power}}{\text{Input microwave power}} \tag{3.16}$$

will be given by:

$$20 \log\left|1/2[1 + \Gamma][3/4\ \beta^3 + 5/8\ \beta^5 + 35/64\ \beta^7 + \ldots + [\frac{{}^{K}C_{K-1}}{2^{K-1}}]\ \beta^K + \ldots]\right|_{K \text{ odd}} \tag{3.17}$$

Equation (3.17) has been derived on the basis of equal sideband components. In practice, the sidebands may not be equal because the circuit admittance and its response may not remain constant over the frequency band, as we have assumed.

3.3 Theoretical Results:

Typical theoretical results were obtained using the device and the circuit admittance data of Figure 2.1. Known points at specific frequencies and r.f. levels were taken and other points at different frequencies were interpolated. The computer was used to calculate Γ and

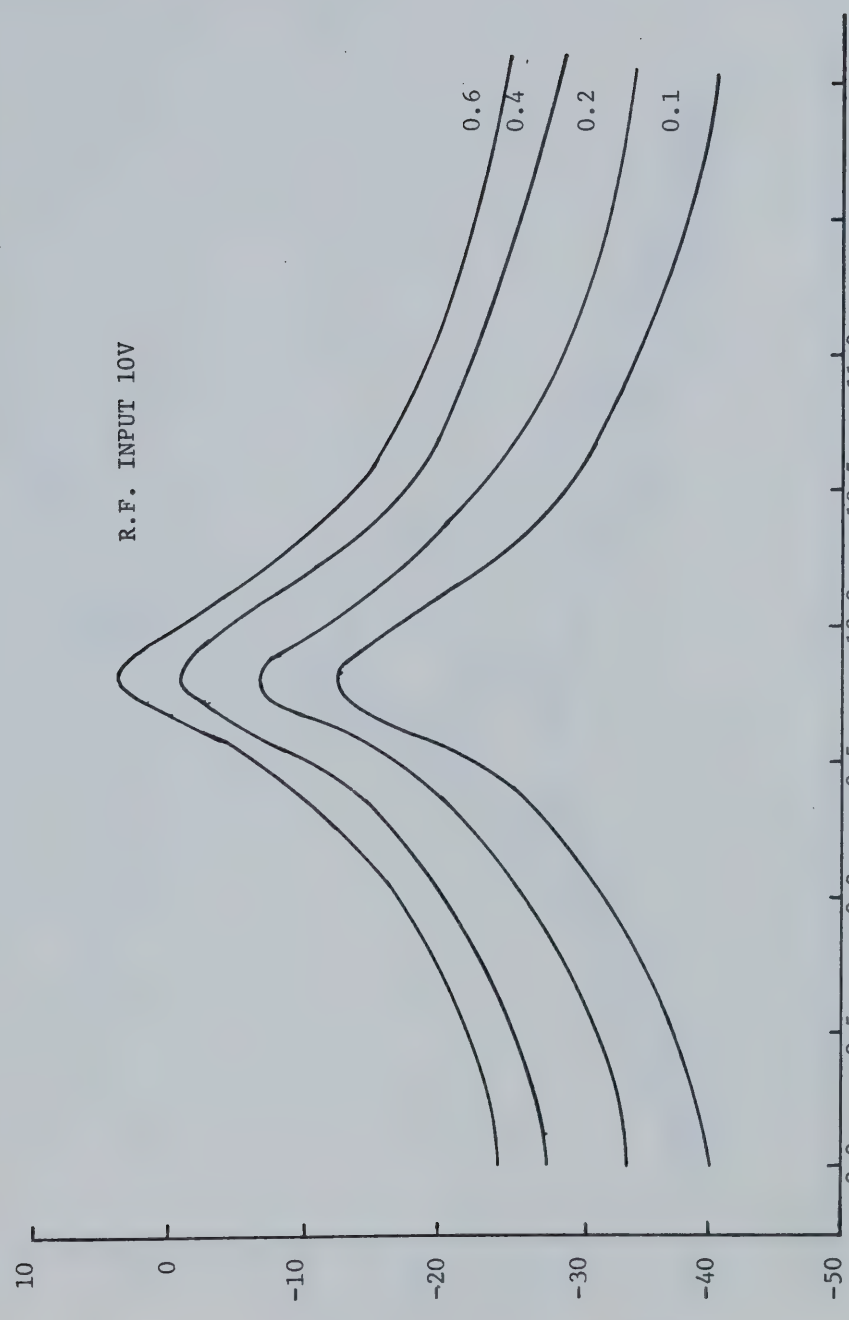

FIG. 3.3 CONVERSION EFFICIENCY VS. FREQUENCY AT DIFFERENT VALUES OF $|Y_{d_1}|$

($|Y_{d_1}|$ = 0.1, 0.2, 0.4, 0.6)

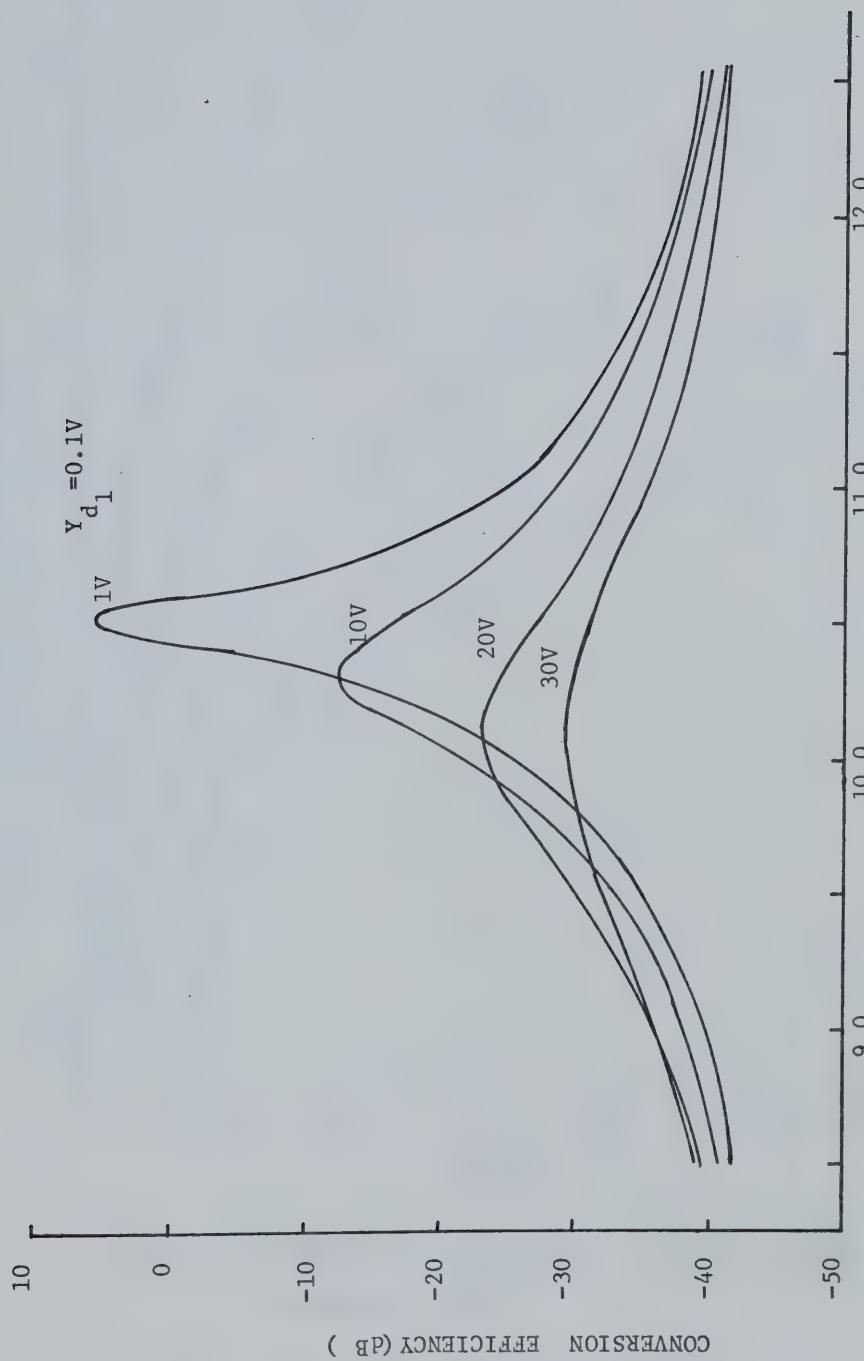

FIG. 3.4 CONVERSION EFFICIENCY VS. R.F. FREQUENCY AT DIFFERENT R.F. POWER LEVELS

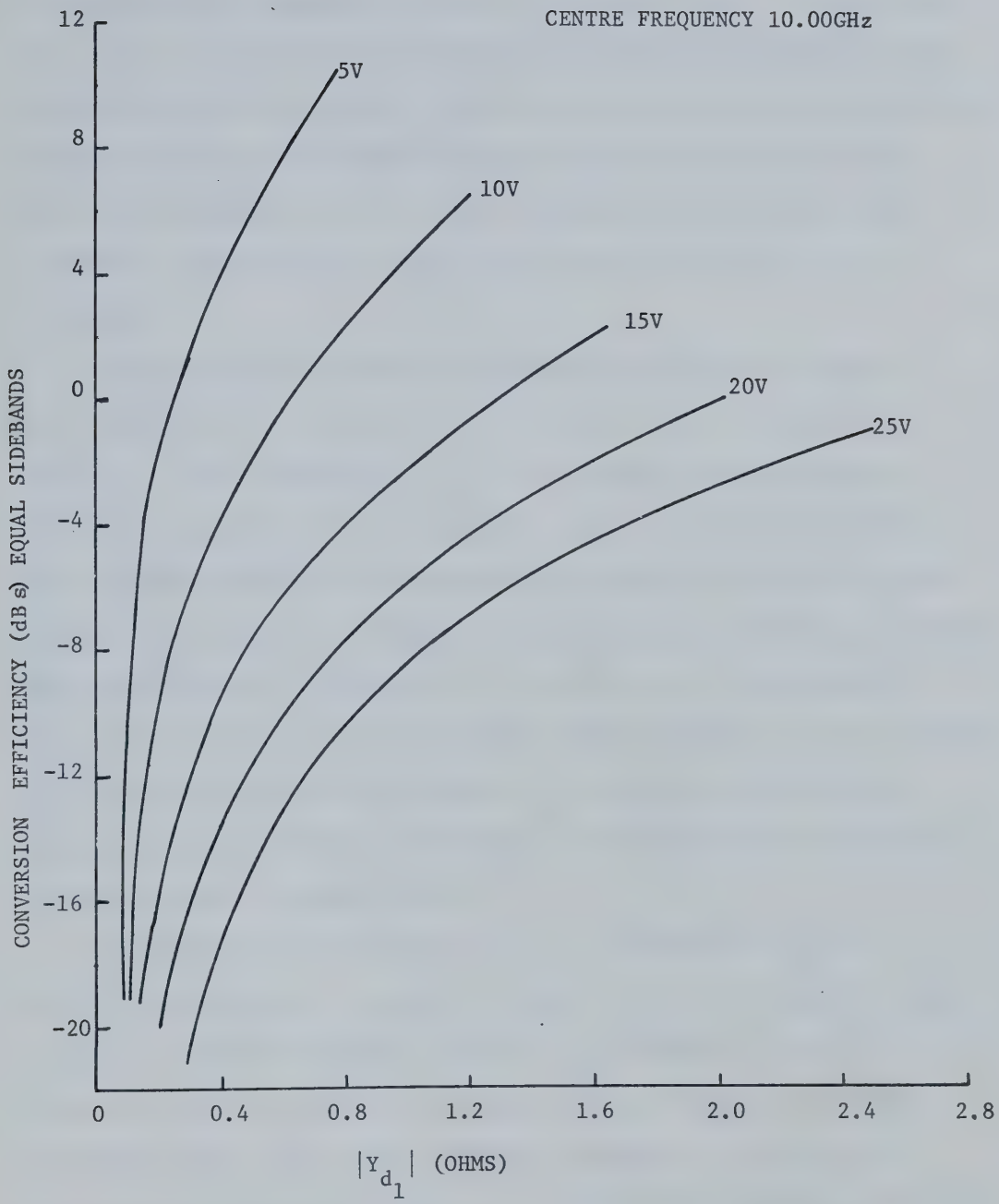

FIG. 3.5 CONVERSION EFFICIENCY VS. $|Y_{d_1}|$ AT DIFFERENT MICROWAVE LEVELS

β for different frequencies at fixed r.f. voltage levels. Using (3.16) and (3.17), the centre frequency gain and conversion efficiency at each frequency were also calculated. The infinite sum of series was considered to have reached its limit when absolute value of increment in (3.16) and (3.17) decreased to 0.01 or less. For all the admittance values considered, this limit was reached with K less than 30 for all the frequencies.

The conversion efficiency or sideband gain for chosen values of $|Y_{d_1}|$ as 0.1, 0.2, 0.4, 0.6 at 10V r.f. signal level is plotted in Figure 3.3. With increasing $|Y_{d_1}|$ or i.f. voltage, the conversion efficiency increases at all frequencies. Also, conversion efficiency curves closely follow the corresponding gain versus frequency characteristics of the amplifier in Figure 2.4. The conversion efficiency versus frequency curves for different r.f. power levels but fixed value of $|Y_{d_1}| = 0.1$, shown in Figure 3.4,confirm this observation. It is interesting to note that a shift in frequencies at which the amplifier has maximum gain for different power levels is also reflected in conversion efficiency versus frequency plots.

The expected conversion efficiency as a function of $|Y_{d_1}|$ at different power levels is plotted in Figure 3.5. It is possible to get a higher conversion efficiency with low $|Y_{d_1}|$ (small i.f. signal level) at smaller microwave (r.f.) power levels. Higher upconverted (sideband) power levels can be obtained at higher r.f. levels, but with reduced conversion efficiency. In a practical amplifier upconverter, therefore, a compromise has to be arrived at for the microwave input level, conversion efficiency and desired upconverted power. Theoretically,

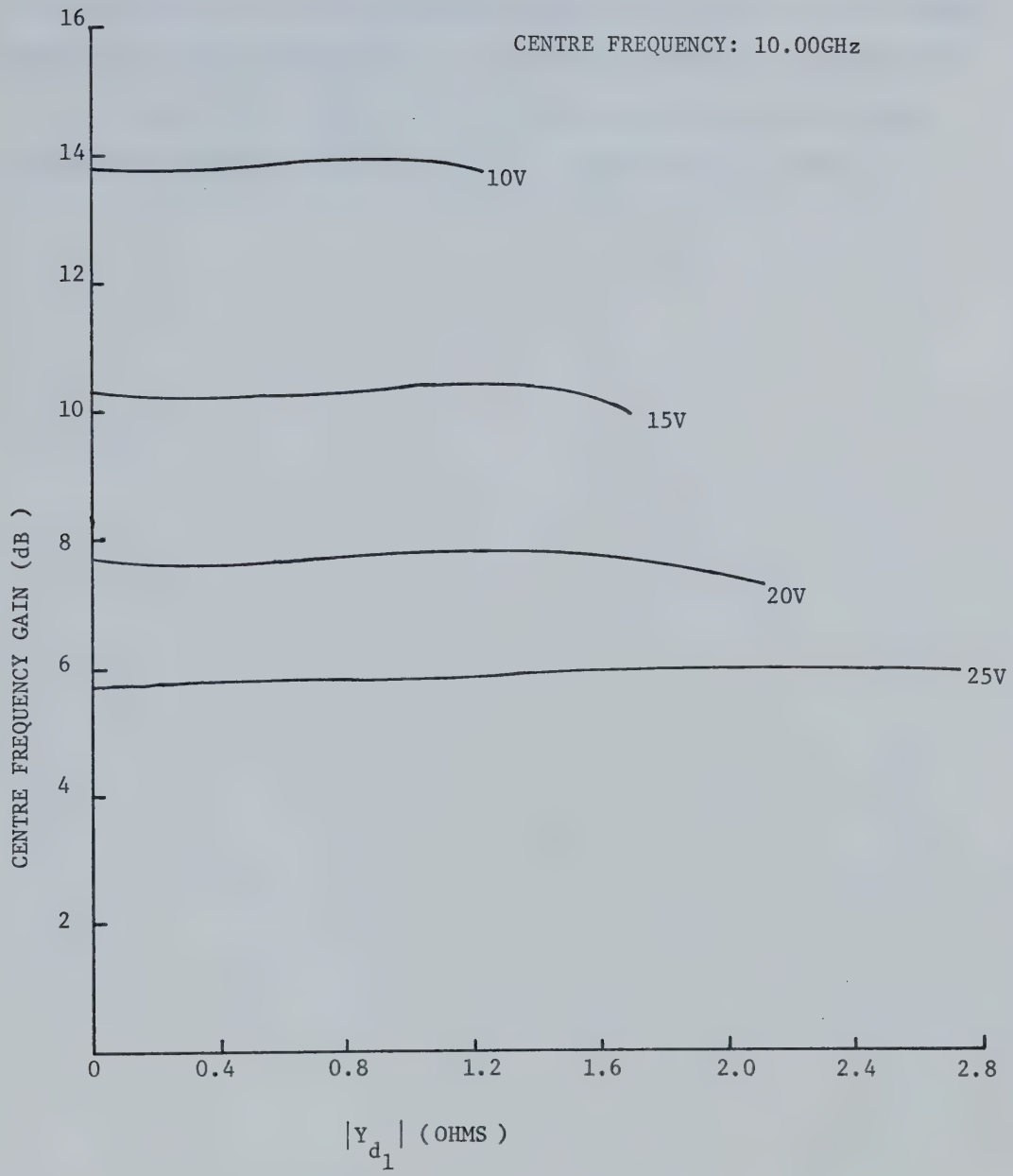

FIG. 3.6 CENTRE FREQUENCY GAIN VS. $|Y_{d_1}|$ AT DIFFERENT INPUT POWER LEVELS

it is possible to have the upconverted output power equal to the maximum power that could be delivered by the diode when acting as an oscillator.

As evident from Figure 3.6, the centre frequency gain also undergoes some change with increasing Y_{d_1} i.e. increasing i.f. level.

CHAPTER IV

EXPERIMENTAL RESULTS FOR IMPATT AMPLIFIER UPCONVERTERS

Experimental results obtained for two X-band Impatt-amplifiers being used as upconverters are presented in this chapter. The results are compared qualitatively with those analysed in the previous chapter and the validity of the theory is discussed.

4.1 Introduction

The measurements of the upconverter characteristics were done using simple and direct measurement techniques explained in section 4.2. Since there are such a large number of parameters (including the physical parameters of the device) on which the converter performance depends, it is impractical to examine the behavior of an upconverter as a function of each one of them. The upconverter performance characteristics were studied as a function of some of the important parameters "external" to the device so as to verify qualitatively some of the results analysed in Chapter III. These "external" parameters include input microwave frequency,input power, the i.f. signal levels and the d.c. bias current. It should be pointed out that the measurements, as presented, were made at the output port of the upconverter.

4.2 Measurement Circuit Used:

The circuit used for measurement of upconverter performance characteristics is shown in Figure 4.1. The circuit is basically the same as used for amplifier measurements, except for the passband filter in the output and the bias circuit of the Impatt-amplifier.

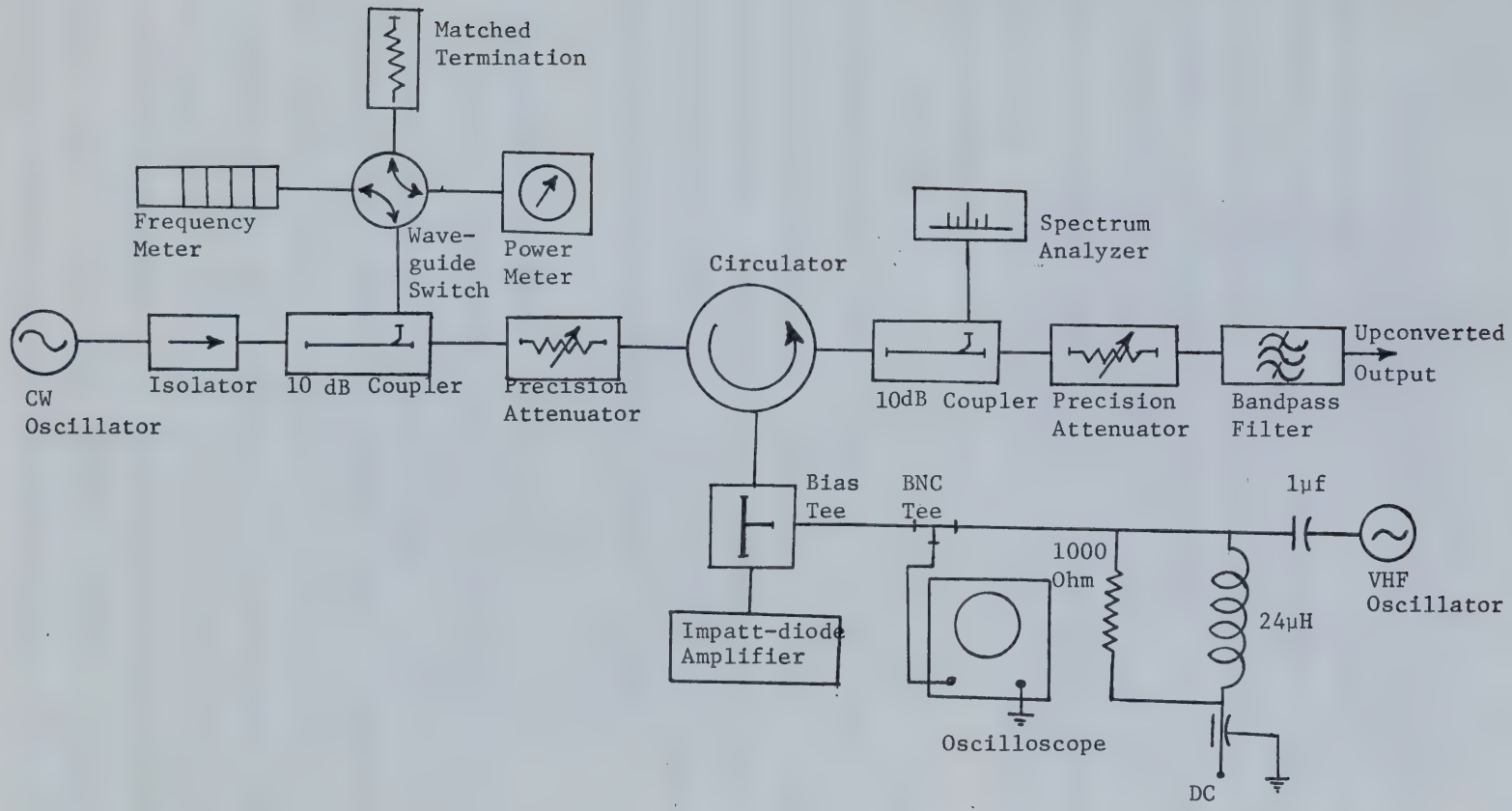

FIG. 4.1 CIRCUIT DIAGRAM FOR MEASUREMENT OF IMPATT AMPLIFIER UPCONVERTER CHARACTERISTICS

The Impatt-device in the coaxial amplifier was biased through a bias tee (Microwave/FXR HW-90N) which has a minimum of 25 db isolation between d.c. and the r.f. For the waveguide amplifier the bias could be directly applied through a BNC connector (UG-1094/U) at the back of the amplifier. D.C. voltage was applied through a 24 μH r.f. choke in parallel with a 1000 ohm resistor. The i.f. signal was applied from a VHF oscillator (hp3200B) through a d.c. blocking capacitor of 1 μf. An oscilloscope (Tektronics 7904) with response up to 1GHz was used to monitor the i.f. levels, via a BNC tee.

Output spectrum and levels of different frequency components were monitored at the output sampling directional coupler. A tunable single cavity narrow band-pass filter could be used to filter out the upconverted (sideband) signal. The filter had an insertion loss of 4dB and 3dB bandwidth of approximately 20MHz. The filter was only used for distortion measurements in section 4.4 where intermediate frequency was 70MHz.

4.3 Experimental Results:

The bias current for almost all the measurements on the single-tuned narrowband coaxial amplifier was maintained at 29.5ma and for the double-tuned waveguide amplifier it was kept at 30ma. The amplifier response is very sensitive to the tuning positions (circuit admittance). During the course of the work small changes occurred in the tuning. To account for these changes and for the purpose of immediate comparison the oscilloscope displays of gain versus frequency plots for both the single tuned as well as double tuned amplifiers are shown in Figures 4.2 and 4.3. The vertical scale was calibrated using the spectrum analyzer and

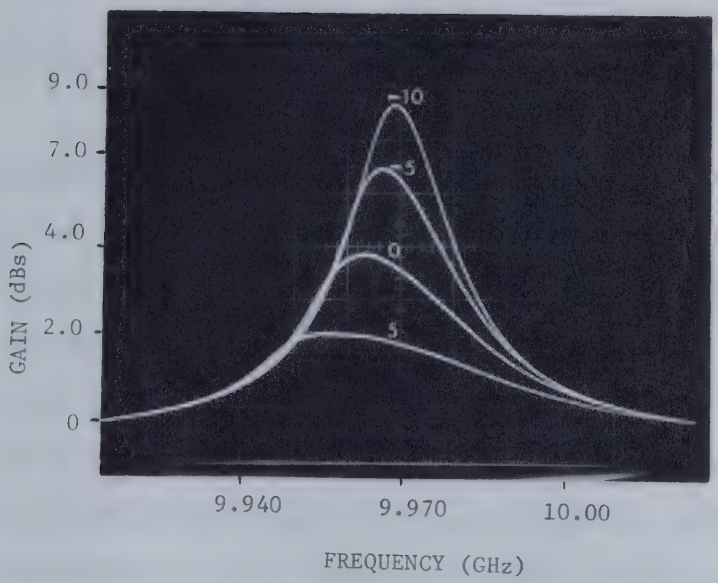

FIG. 4.2 OSCILLOSCOPE DISPLAY OF GAIN VS. FREQUENCY CHARACTERISTICS AT DIFFERENT INPUT LEVELS (SINGLE-TUNED AMPLIFIER)

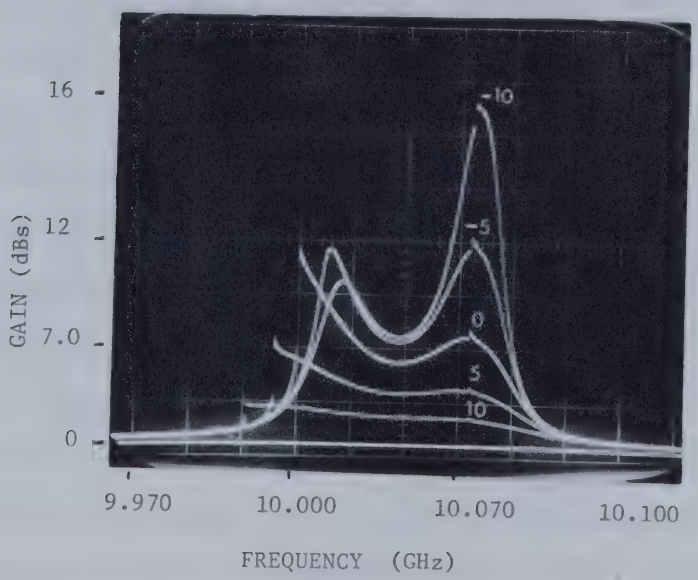

FIG. 4.3 GAIN VS. FREQUENCY CHARACTERISTICS AT DIFFERENT INPUT LEVELS (DOUBLE-TUNED AMPLIFIER)

INPUT LEVELS ARE IN dBm

is not linearly related to the gain in dbs.

4.3.1 Single-tuned Amplifier Upconverters:

The i.f. frequency for most of the measurements, was selected to be 10MHz so that the theoretical assumption that circuit admittance is almost constant in the band of centre frequency and first order sidebands holds within reason.

Lower sideband (LSB) conversion efficiency as a function of microwave frequency at different input power levels is plotted in Figure 4.4. A small-signal i.f. voltage of 0.2V peak to peak (V_{pp}) was selected. The plots compare very well with the amplifier gain characteristics of Figure 4.2 and qualitatively with theoretical results in Figure 3.3. The shift in frequency at which the maximum efficiency (gain) occurs, and increase in bandwidth with increase in signal levels is quite apparent. A maximum conversion efficiency of -2dB is observed. For higher i.f. levels, however, this efficiency increases.

The increase in upconversion efficiency with increase in i.f. level is evident in plots of Figure 4.5. A microwave input of -5dbm was selected as a compromise between small and large microwave signal levels. The i.f. signal levels of 0.1, 0.2, 0.4, 0.6 Volts (peak to peak) were chosen for comparison of these results with those theoretically obtained in Chapter III. Except for i.f. level of 0.6 volts the results are in a very good qualitative agreement with theoretical broadband results in Figure 3.1. At 0.6 V_{pp} the 'dip' at a frequency of 9.950GHz might have been caused because of some higher order admittance variation components becoming prominent or due to local change in device admittance characteristics at that frequency. A shift in frequency where maximum of conversion

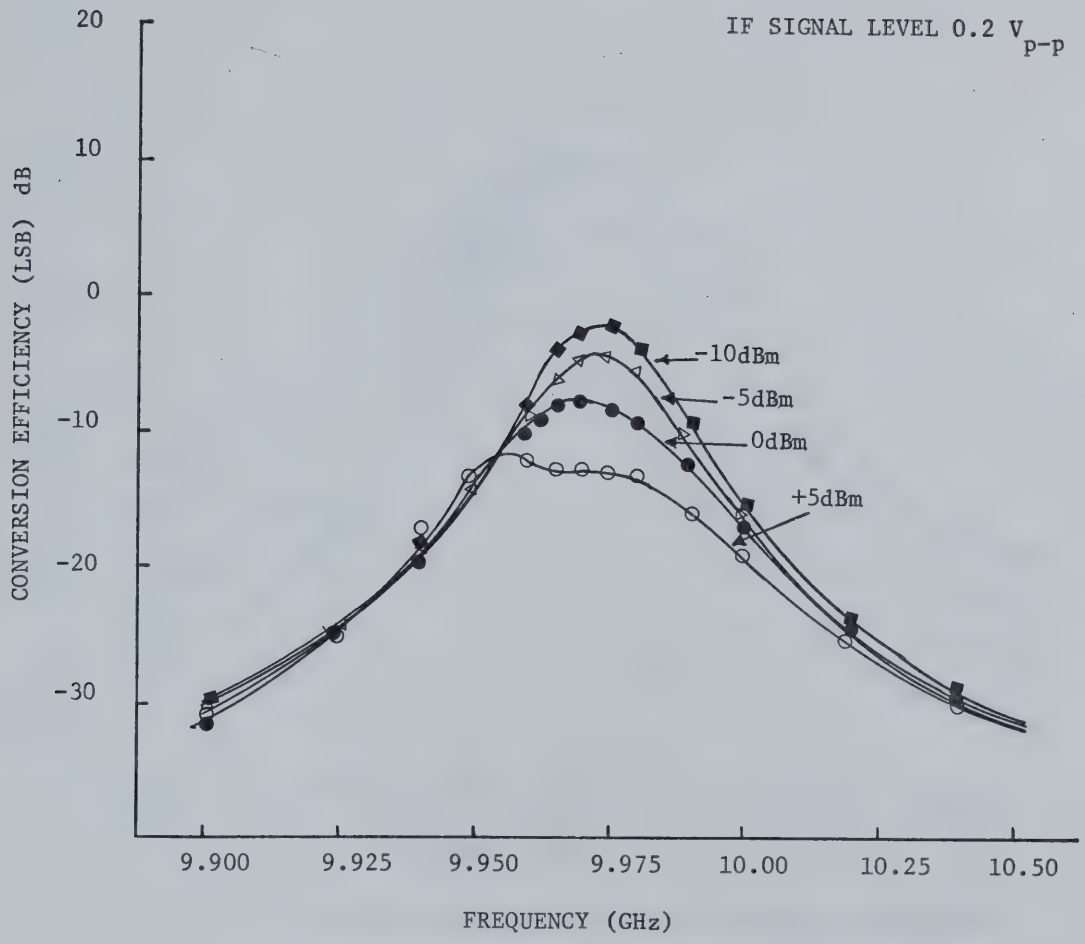

FIG. 4.4 CONVERSION EFFICIENCY (LSB) VS. MICROWAVE FREQUENCY AT DIFFERENT INPUT LEVELS

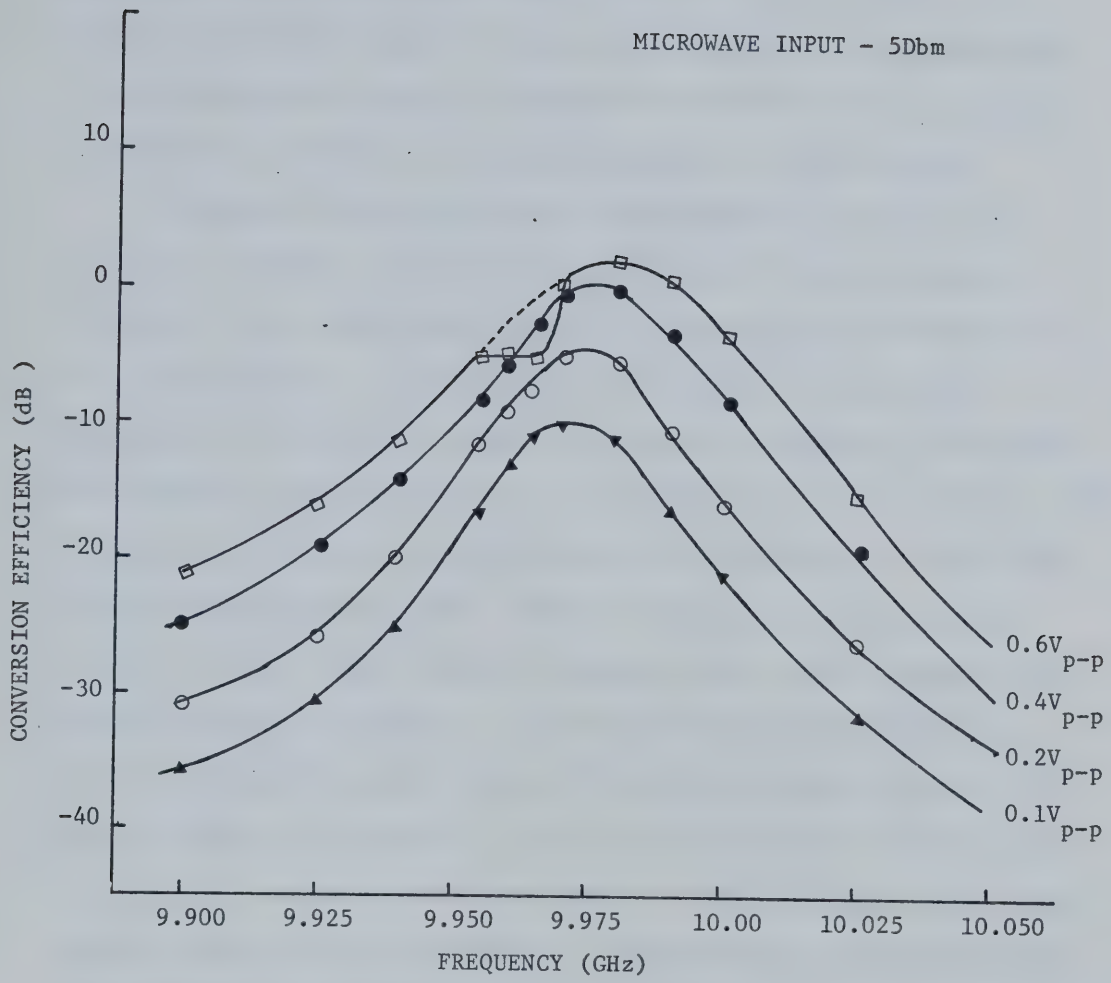

FIG. 4.5 CONVERSION EFFICIENCY (LSB) VS. MICROWAVE FREQUENCY AT DIFFERENT I.F. VOLTAGE LEVELS

efficiency occurs at different power levels is also noticeable. The shift becomes more prominent at higher i.f. levels. This suggests that there is indeed some change in admittance characteristics due to large i.f. signal, an effect that has been neglected in the analysis.

The change in device-admittance characteristics and hence the frequency of maximum conversion efficiency is more clearly evident in Figure 4.6. This figure represents plots of conversion efficiency versus i.f. signal levels. At small signals the microwave frequency was adjusted to the frequency at which the gain of the amplifier was maximum. The conversion efficiency curves for small microwave inputs (-10dBm, -5dBm) follow the theoretically expected curves for very small i.f. after which the curves start droping down. When the microwave frequency was re-adjusted so that centre frequency component again could be maximum the dotted curves were obtained. These follow the theoretically expected curves. At larger microwave inputs (0dBm, 5dBm) results are similar to those theoretically expected. It is interesting to note from the curves that the i.f. levels at which this change in characteristics takes place, depend upon microwave input level. It is reasonable to conclude from these observations, therefore, that the analysis presented in the previous chapter is applicable for very strong microwave pump signals only.

Lower side band was used for calculation of conversion efficiency for all the plots discussed above. The choice of LSB was arbitrary. Any convenient sideband can be used for the output. As is quite apparent from Figure 4.7, USB can be bigger in magnitude than LSB depending upon input microwave frequency. The inequality of sidebands may be due to circuit admittance at sideband frequency being different from circuit admittance at centre frequency. It is worth noticing that sidebands are

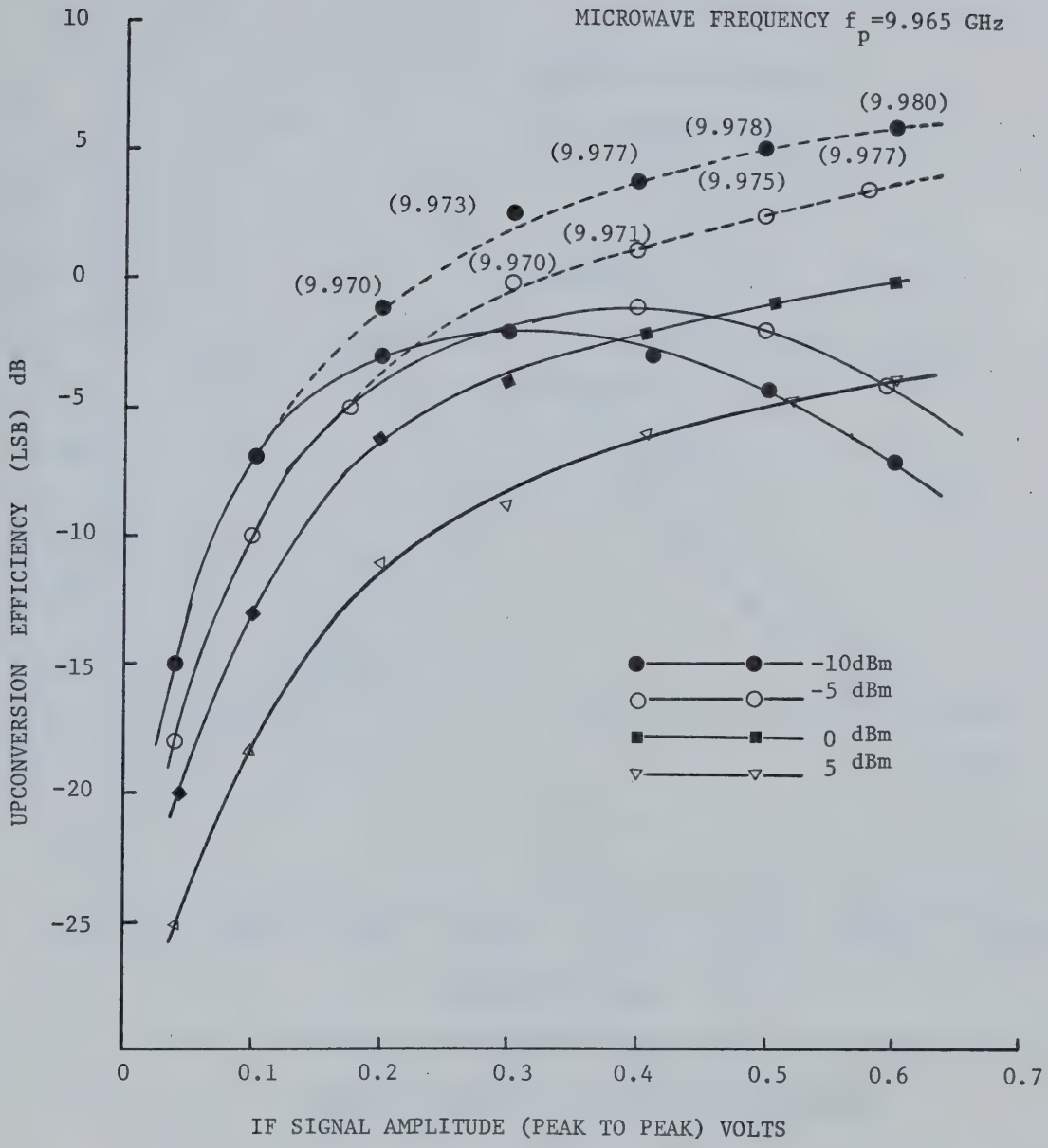

FIG. 4.6 CONVERSION EFFICIENCY (LSB) VS. I.F. SIGNAL AMPLITUDE AT DIFFERENT INPUT POWER LEVELS

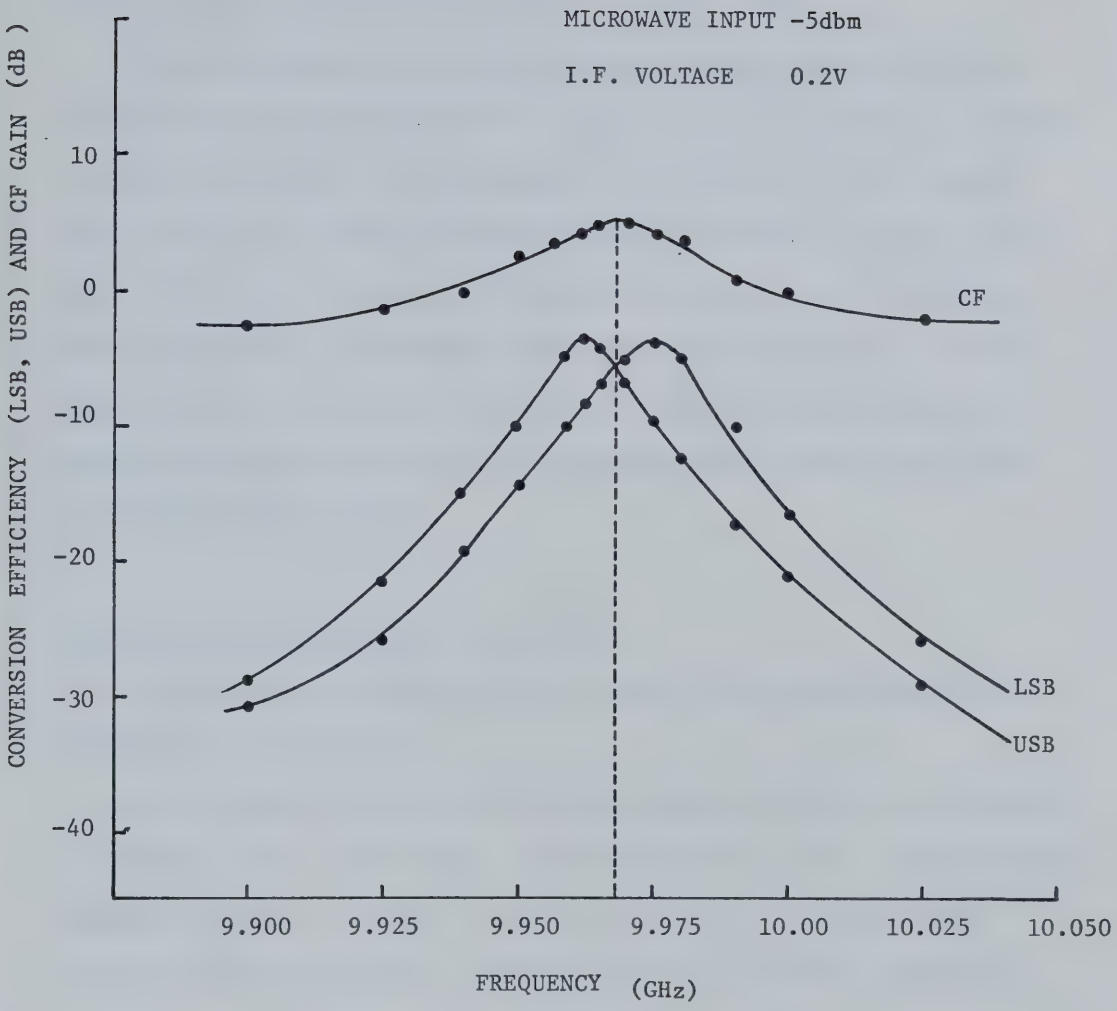

FIG. 4.7 CONVERSION EFFICIENCY (LSB AND USB) AND CENTRE FREQUENCY GAIN VS. INPUT MICROWAVE FREQUENCY

equal when microwave frequency is adjusted where peak of CF gain occurs. Also, the maximas of the LSB and USB are displaced exactly by intermediate frequency from this centre frequency, on either sides.

Lower and upper sideband magnitudes as a function of d.c. bias current are plotted in Figure 4.8. The microwave frequency was adjusted so that the amplifier had maximum gain (at 29.5ma d.c. bias current). The saturation of sideband components with bias current, similar to the power saturation in Impatt-amplifiers can be observed. The amplifier being narrow-band in frequency, measurements for varying i.f. were not done because as the microwave frequency or the components fall out of amplification band, the sidebands become very small (less than -20dBm at -5dBm microwave input).

4.3.2 Double-tuned Amplifier Upconverter:

A second set of measurements was taken on the relatively broad-band waveguide amplifier.

Lower sideband conversion efficiency versus the microwave frequency at different input power levels is plotted in Figure 4.9. Intermediate frequency was kept as 10MHz at a level of $0.5V_{p-p}$. The bandwidth characteristics in the plots closely follow the amplifier gain plots in Figure 4.3. The double peaks and decrease in efficiency with extended bandwidth for higher microwave inputs are also noticeable.

The intermediate frequency for all the experimental results discussed so far was 10MHz. This was done in order to verify the analysis of Chapter III. In practical microwave upconverters, however, much higher i.f. (70-140MHz) is used. The rest of the measurement data for the

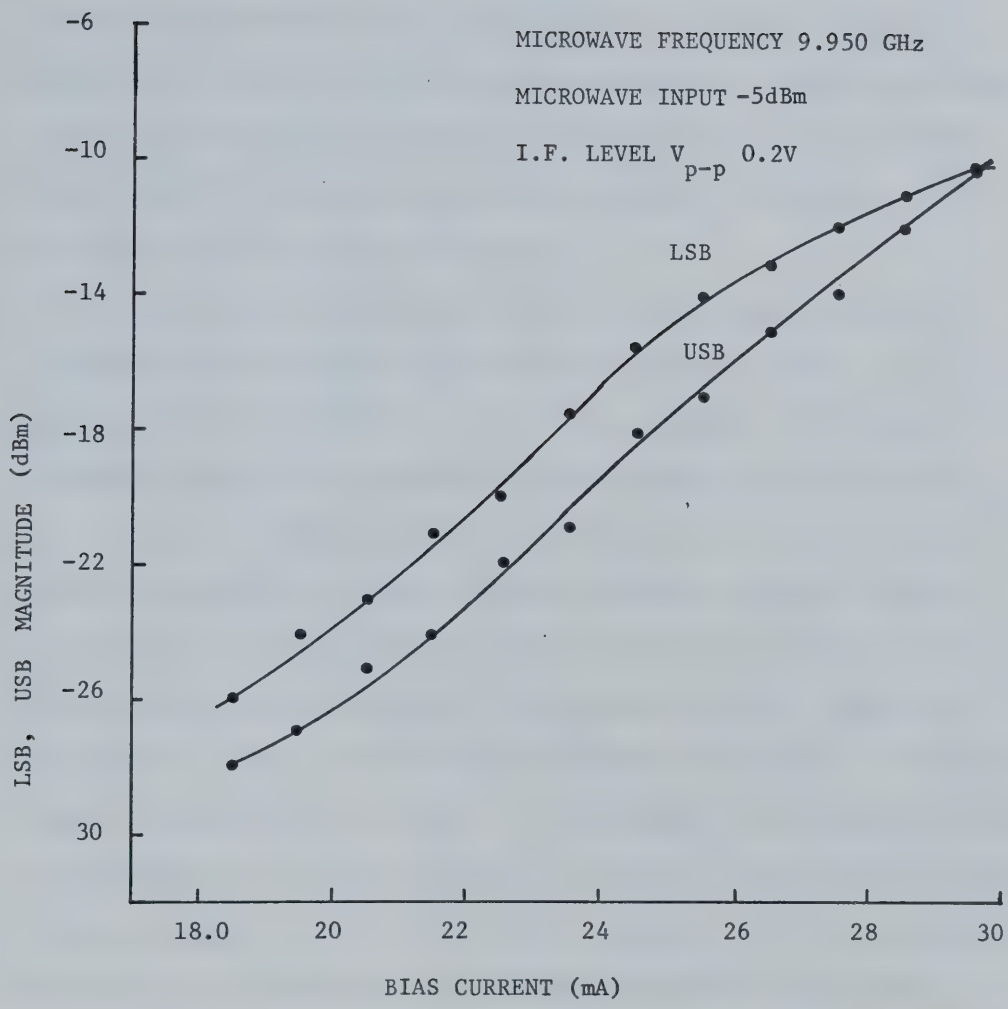

FIG. 4.8 LOWER AND UPPER SIDEBAND MAGNITUDES VS. BIAS CURRENT

broadband amplifier, therefore, was obtained at 70MHz i.f. Figure 4.10 shows the LSB magnitude versus input microwave power plots at different microwave frequencies. The saturation of sideband power in the up-converter at increased input power seems to be similar to saturation properties of Impatt-amplifier shown in Figure 2.9. At 0dbm input, the sideband power increases to 9dBm at 10.075 GHz input. These results indicate that the upconverter performance behavior is similar to the amplifier performance characteristics.

LSB conversion efficiency versus i.f. peak to peak voltage at different input microwave power levels is plotted in Figure 4.11. A maximum conversion efficiency of 13 dB was obtained. The curves are in remarkable qualitative agreement to those expected upto about $0.7V_{p-p}$ i.f. level. The efficiency curves start departing from the expected behavior at higher i.f. levels, possibly because of shift in device admittance characteristics as already explained in section 4.3.1. It is to be noticed that this departure from expected behavior takes place at higher i.f. levels in broad-band amplifiers as compared to narrow-band case. The LSB magnitude versus i.f. voltage plots at different microwave input frequencies, shown in Figure 4.12, indicate that maximum LSB power output is available for 10.075GHz input frequency. At this microwave frequency the LSB component (at frequency 10.005GHz) falls at the amplifier gain peak as is evident in Figure 4.3.

In Figure 4.13, the LSB, USB and centre frequency components as a function of input microwave frequency are plotted at an input level of -5dBm. The side-bands are equal when the microwave input frequency is in the centre of the amplifier band. The results indicate that the

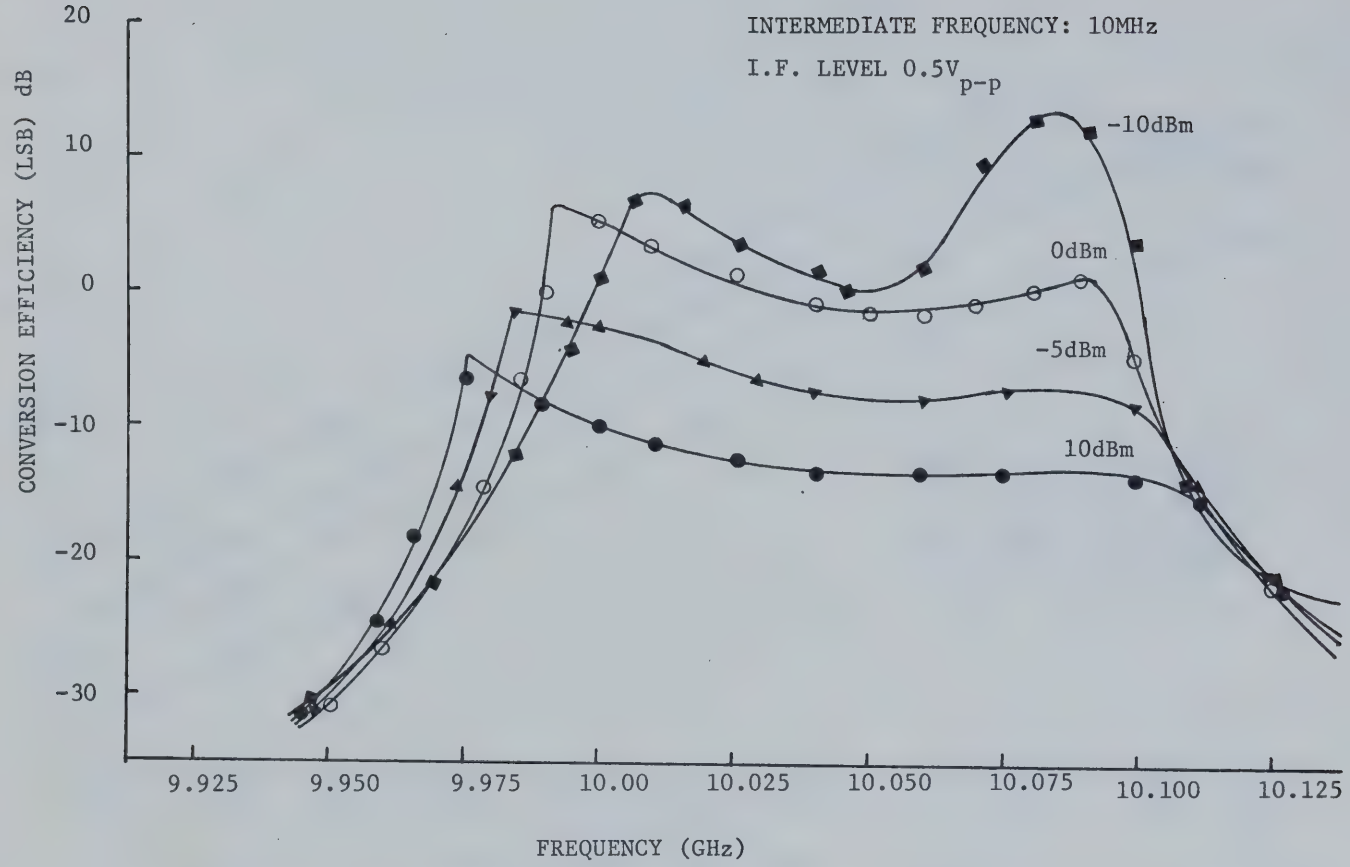

FIG. 4.9 CONVERSION EFFICIENCY (LSB) VS. INPUT FREQUENCY AT DIFFERENT INPUT POWER LEVELS (DOUBLE TUNED AMPLIFIER)

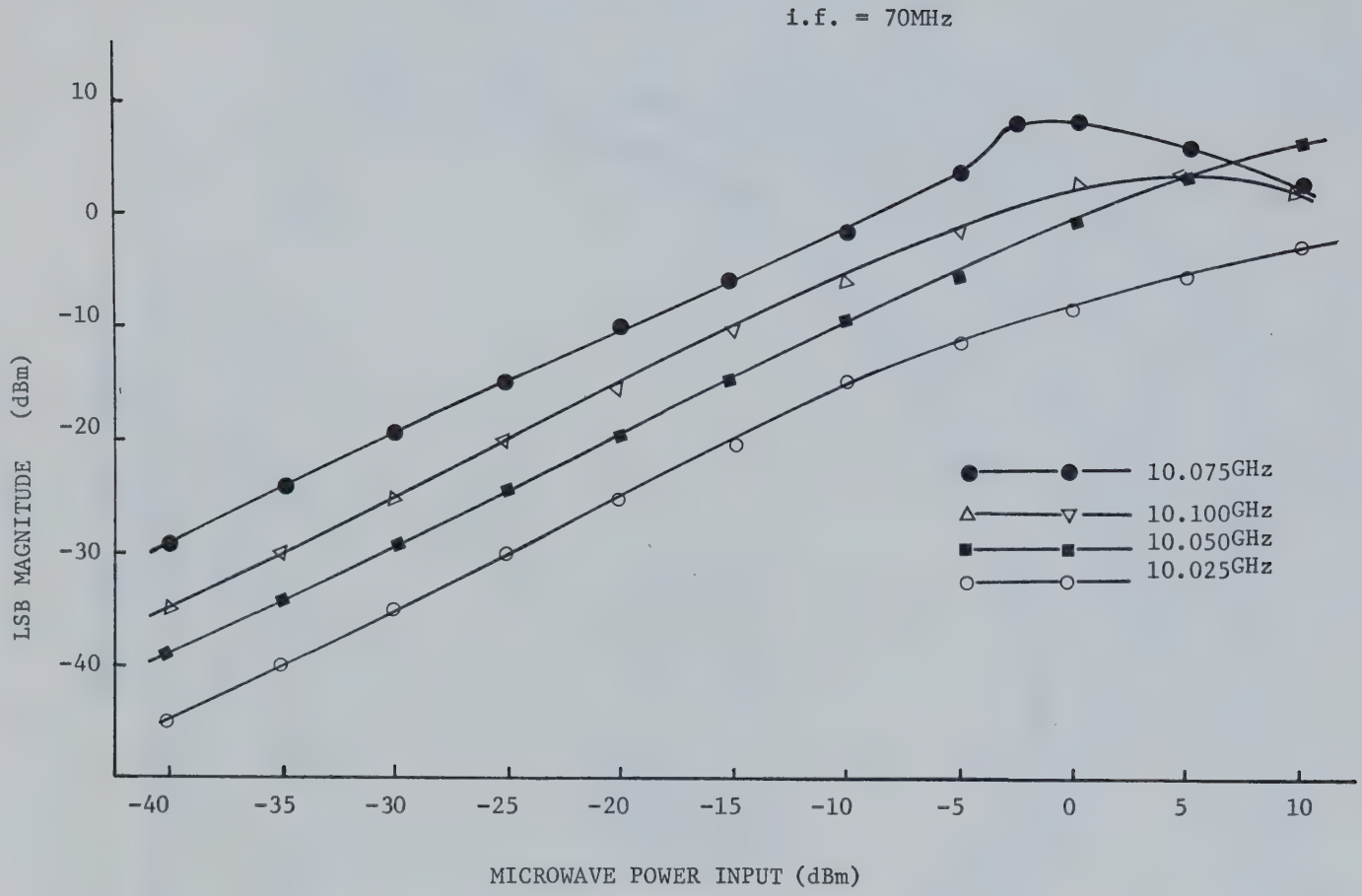

FIG. 4.10 LOWER SIDEBAND MAGNITUDE VS. INPUT MICROWAVE POWER AT DIFFERENT INPUT FREQUENCIES

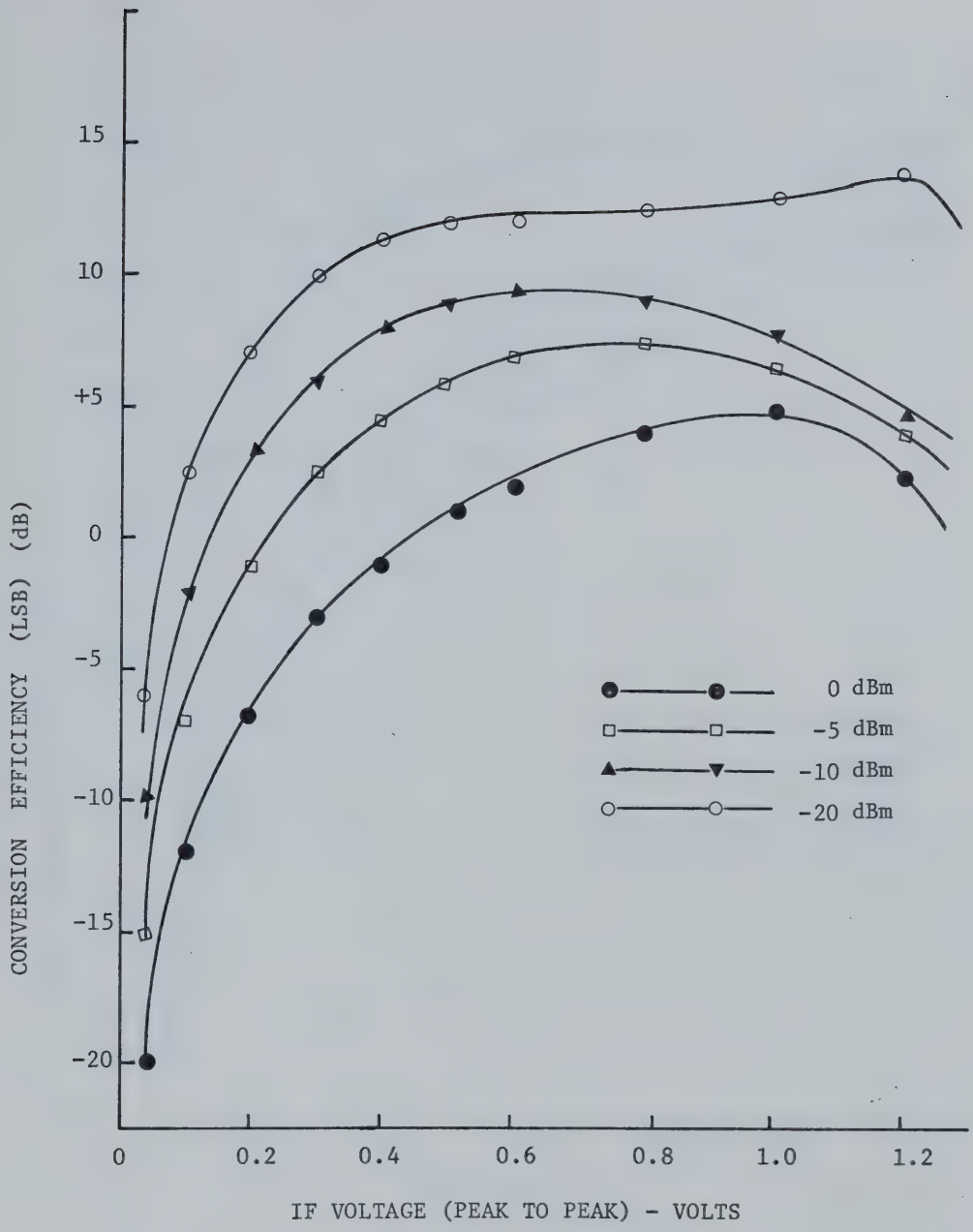

FIG. 4.11 UPCONVERSION EFFICIENCY VS. I.F. VOLTAGE INPUT AT DIFFERENT INPUT POWER LEVELS

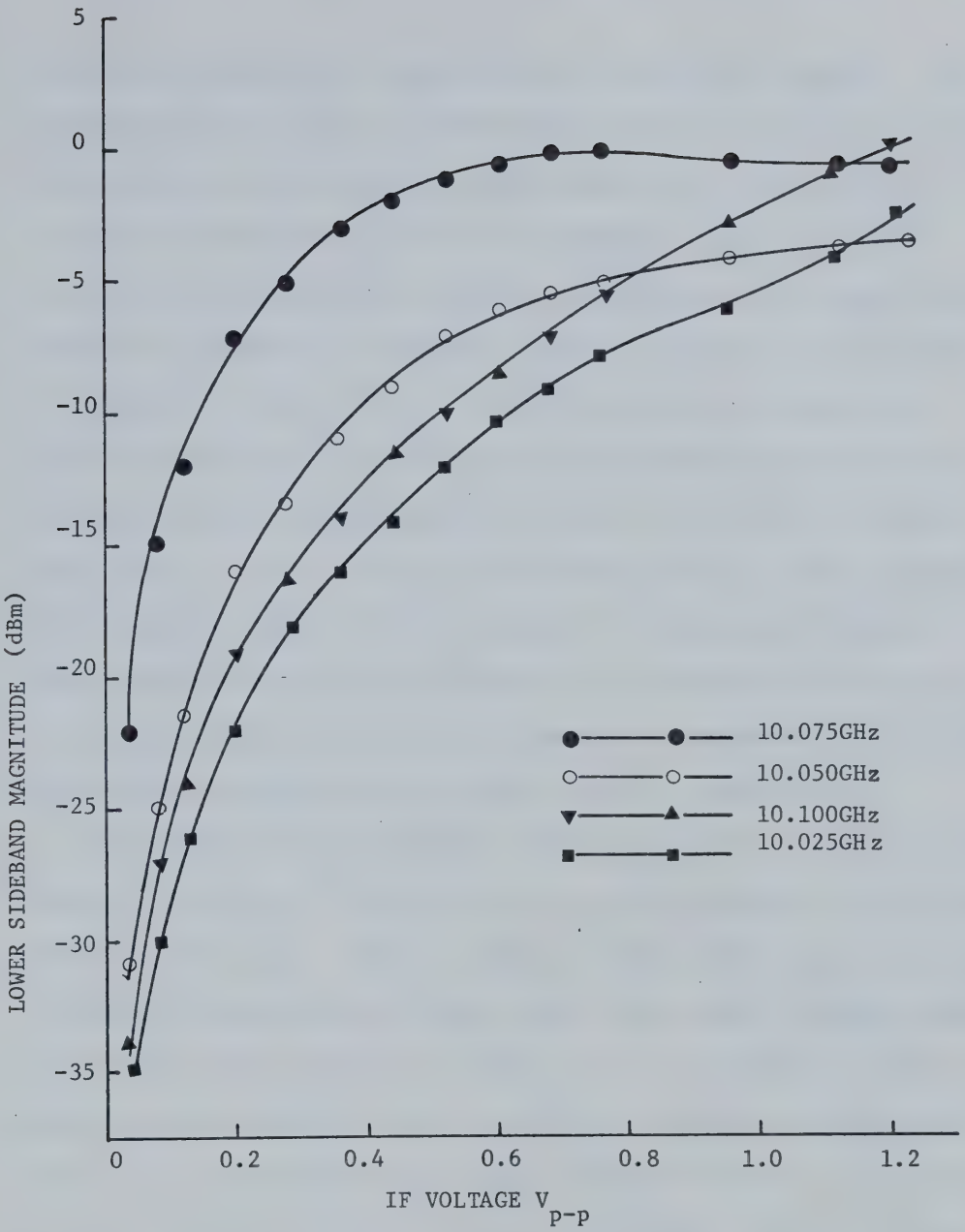

FIG. 4.12 LOWER SIDEBAND MAGNTIUDES VS. I.F. VOLTAGE AT DIFFERENT INPUT FREQUENCIES

upconversion band width is smaller than the amplifier bandwidth. Also, the component magnitudes are maximum when both centre frequency and sideband components fall within the amplification band of the amplifier. It can also be observed that when the microwave frequency is within the amplification band of the amplifier (larger gain) the change in the magnitude of sidebands is relatively slow as compared to the drop when it is outside the band. This is rather an interesting observation because in equation (3.17) that gives sideband magnitudes $[1 + \Gamma]$ is a multiplying factor in the expression, where Γ is the centre frequency voltage gain. It can be concluded from these plots and above discussion that sideband response of the upconverter is determined by both the centre frequency gain of the amplifier and the response of the microwave circuit at component frequencies. A maximum of upconverted power (sideband) can be obtained by optimization of both of these values.

In Figure 4.14, upper sideband (USB) magnitudes as a function of USB frequency are plotted. Various fixed microwave frequencies were selected while i.f. was varied. For r.f. frequency outside the amplification band (9.950GHz), lower sideband response remains very small (less than -35dbm) and the USB response follows the gain curve of the amplifier, with its maximum magnitude being -12dbm. At the r.f. frequencies closer to the centre of the amplification band (higher CF gain) the USB response goes up, still following the gain curve of the amplifier. Similar behavior was observed when the r.f. frequency was tuned towards the upper end of the amplification band and LSB response was observed. The dependence of sideband magnitude on centre frequency gain is quite apparent. Also, when a frequency modulated i.f. signal is impressed upon the bias of the amplifier, f.m. to a.m. conversion is expected to be small because of

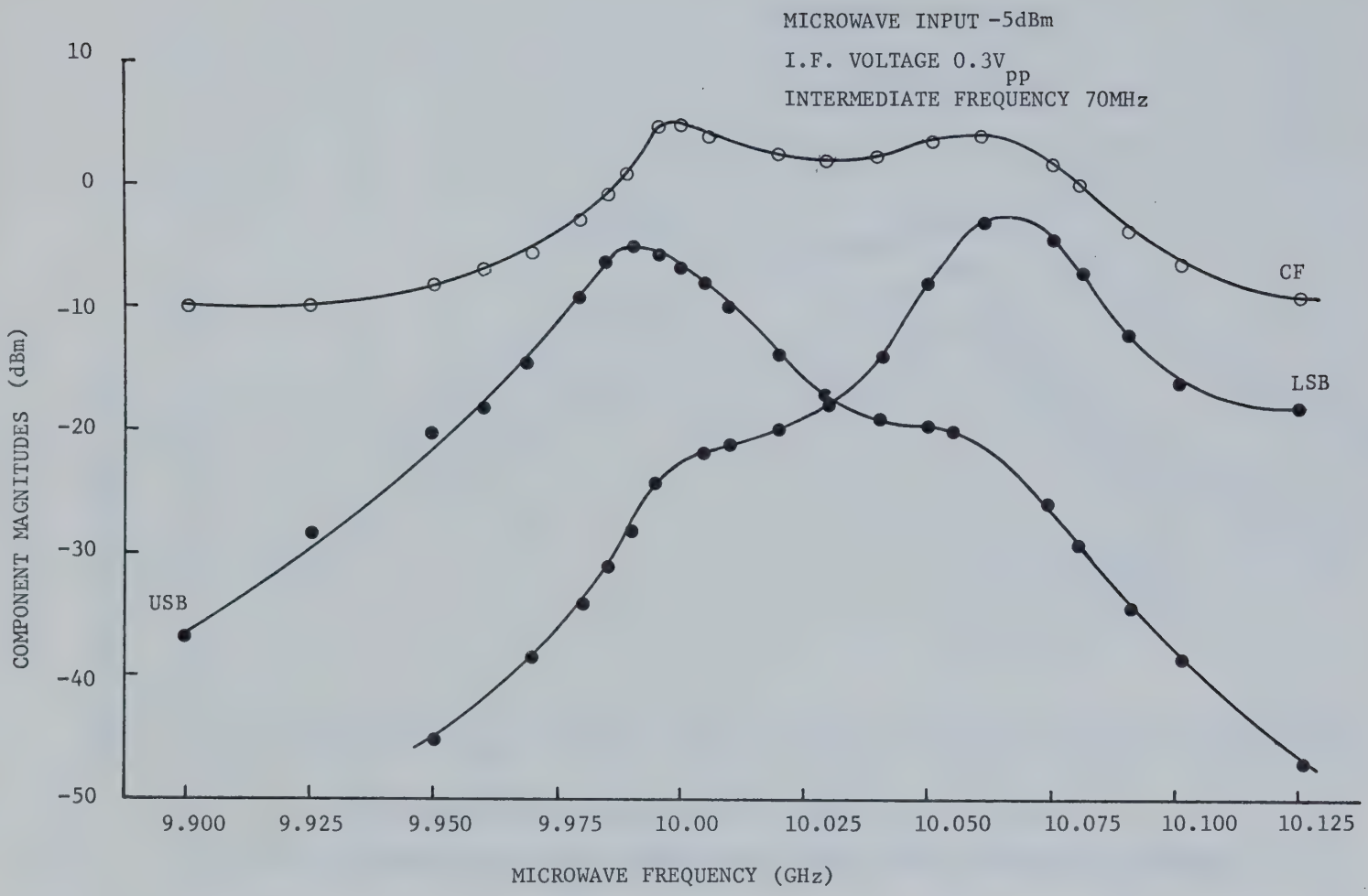

FIG. 4.13 LSB, USB, CENTRE FREQUENCY COMPONENT MAGNITUDES VS. INPUT MICROWAVE FREQUENCY

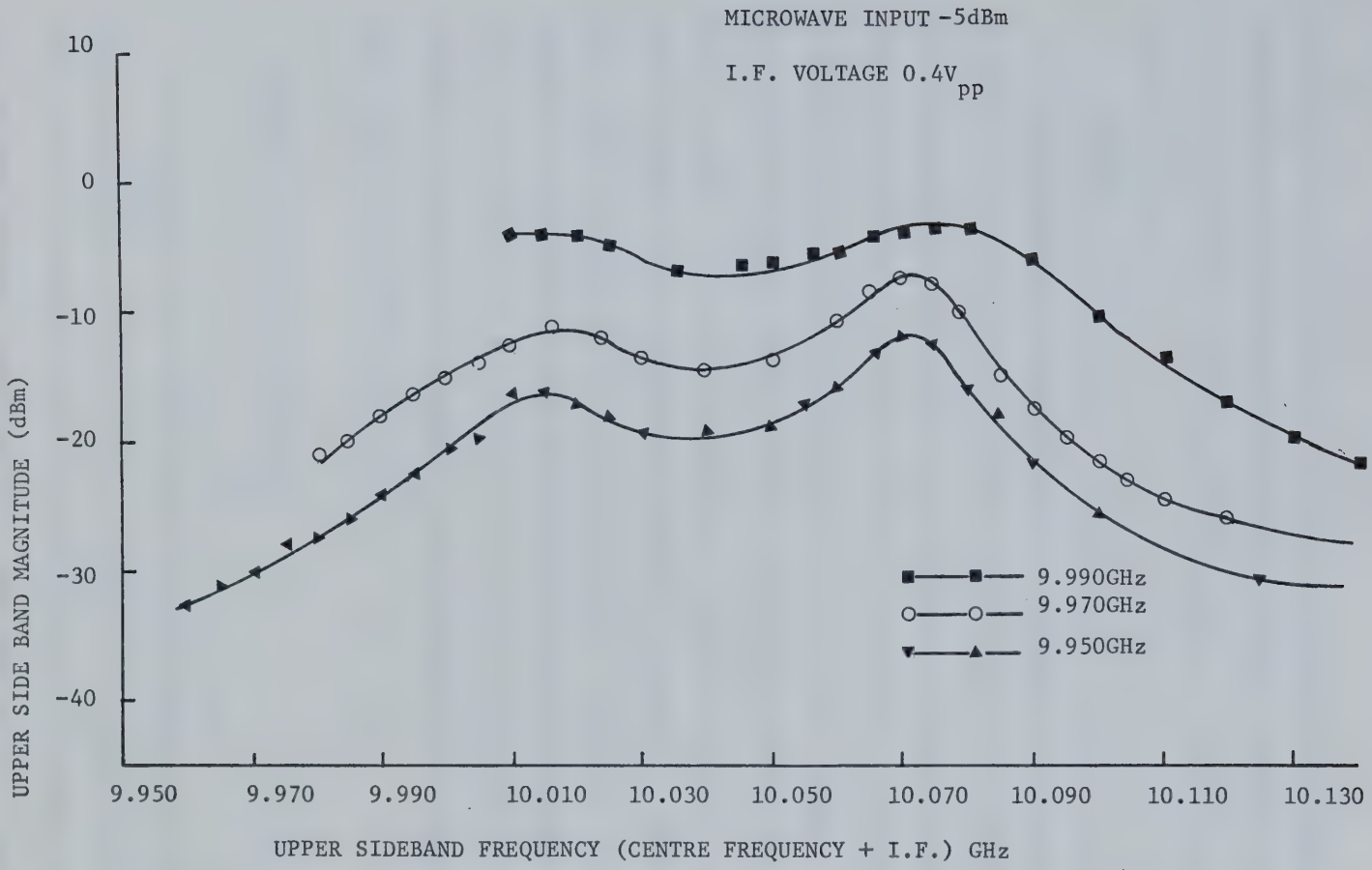

FIG. 4.14 USB MAGNITUDE VS. USB FREQUENCY FOR FIXED CENTRE FREQUENCY AND VARYING I.F.

wideband upconversion response. At input frequency of 9.990GHz, the response variations remain within 3db over the total amplifier band. The performance should further improve by making the amplifier response flatter.

According to the analysis in Chapter III, the sideband generation in the bias-modulated Impatt-amplifiers is expected to be mainly due to gain magnitude variations with the applied signal. To verify this, the experimental set up of Figure 4.15 was used to directly compare the sideband magnitudes as seen from the spectrum analyzer with those expected from oscilloscope display of crystal detector output. It is to be noted that crystal diode will detect only the magnitude variations in the r.f. signal. The calibration curve of the diode detector, namely, the plot between d.c. voltage output and $\sqrt{P_{in}}$, where P_{in} is microwave input power, was observed to be a straight line. The output of the detector for varying r.f. amplitude would be as shown in Figure 4.16. The expected sideband magnitude for a.m. can be directly calculated in dBs from the output d.c. voltage V_{dc} and the detected i.f. magnitude V_{ac}, by using the following expression:

$$\text{Sideband Magnitude} = 20 \log \frac{V_{ac}}{2V_{dc}} \qquad (4.1)$$

The measurements were made using a low bias-modulation frequency (1MHz) because of detector frequency response. The saturation of the diode could be avoided by precision attenuator in the output circuit. The calculated sideband magnitudes and those measured on the spectrum analyzer are shown in Table 4.1. Measurements at 10.070GHz for different microwave input and i.f. levels indicate that measured values are

comparable within 1dB with those expected. However, at 10.005GHz the measured values are observed to be upto 5dB greater than those expected. This suggests that at this microwave frequency, the r.f. signal could be frequency (phase) modulated because of applied i.f., which would make an additional contribution to the sidebands.

A frequency discriminator,in the place of crystal detector was used to test the presence of f.m. After application of bias signal some signal was detected at the output of the discriminator, which increased with increasing i.f. level. This indicates that the bias modulation could cause the susceptance of the device to vary with the signal frequency, depending upon the point of operation in the admittance plane. Any further analysis on the topic should take this factor into consideration. The contribution to the sideband component due to frequency (phase) modulation is not necessarily undesirable. The important criterion for the upconverter to be used in system applications is the amount of distortion it introduces in the signals modulated on the i.f. For flat response upconverters, the a.m. distortion in frequency modulated signals on the i.f. is expected to be small, as discussed in section 4.3.2.

4.4 Signal Distortion in Impatt-amplifier Upconverters

The nonlinear saturation mechanism of the sideband components as observed in Figure 4.10 should be expected to cause signal amplitude and phase distortions in the upconverter at higher microwave input levels. The studies of distortion introduced by Impatt-amplifier upconverters in the amplitude and frequency modulated signals on the i.f. are important

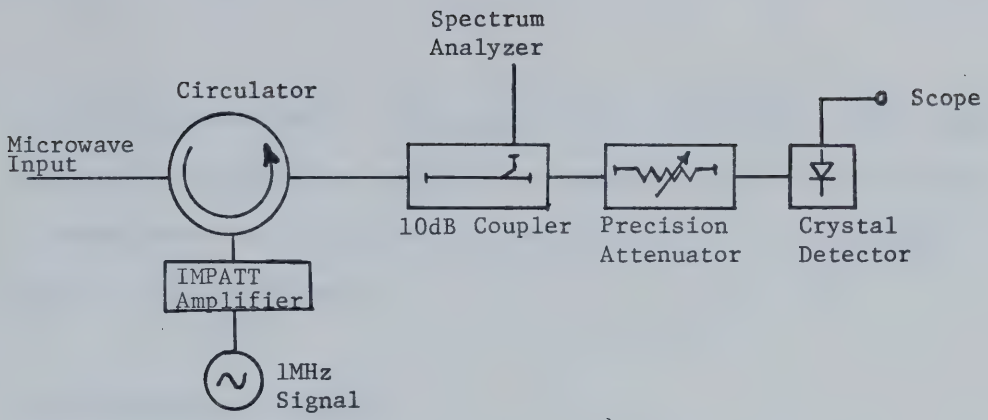

FIG. 4.15 A.M. DETECTION OF BIAS MODULATED SIGNAL

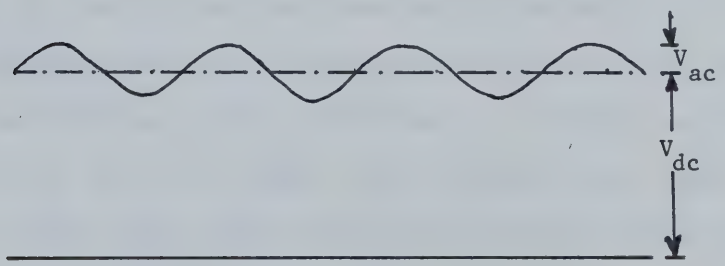

FIG. 4.16 OSCILLOSCOPE DISPLAY OF THE DETECTED SIGNAL

TABLE 4.1 SIDEBAND MAGNITUDE FROM SPECTRUM ANALYZER AND OSCILLOSCOPE MEASUREMENTS

Frequency →	10.070 GHz				10.005 GHz			
i.f. level →	0.05 V_{pp}		0.10 V_{pp}		0.05 V_{pp}		0.10 V_{pp}	
↓ Microwave Power	Expected dBm	Measured dBm	Expected dBm	Meas. dBm	Expec. dBm	Meas. dBm	Expec dBm	Meas. dBm
-10dbm	-29.9	-31.0	-24.7	-25	-32.6	-30.0	-27.2	-23.0
- 5dbm	-32.0	-32.5	-25.4	-26	-33.0	-29.0	-24.7	-20.0

for system applications. But,because of nonavailability of VHF source with f.m., the distortion test for f.m. signals could not be performed. An experimental investigation into the distortion for an amplitude modulated signal was made.

4.5.1 Measurement Circuit:

The measurement circuit was the same as shown in Figure 4.1, with a few additions. An amplitude modulated i.f. was applied at the bias circuit. The audio signal modulated on r.f. was detected by using a crystal detector (HPX424A) at the narrow pass-band filter output. It was assumed that the detector diode does not introduce significant distortion in the output signal. Both the input audio signal and detected output signal could be directly compared on the oscilloscope. By using a low frequency spectrum analyzer (Systron Donner 710/800) the second and third harmonics of the audio signal could be measured.

4.5.2 Experimental Results:

A frequency of 10KHz was used for amplitude modulation of the intermediate frequency of 70MHz. Input microwave frequency of 10.073GHz was selected so that the LSB (at 10.003GHz) was maximum. The filter was tuned to this frequency and the distortion was studied in terms of harmonic contents. The input microwave signal was varied to different levels. The third harmonic was always more than 50db below the fundamental. The second harmonic contents are plotted in Figure 4.17. A minimum is observed at -10dBm input. Harmonic contents increase with increased input levels as expected. In Figure 4.18 the relative

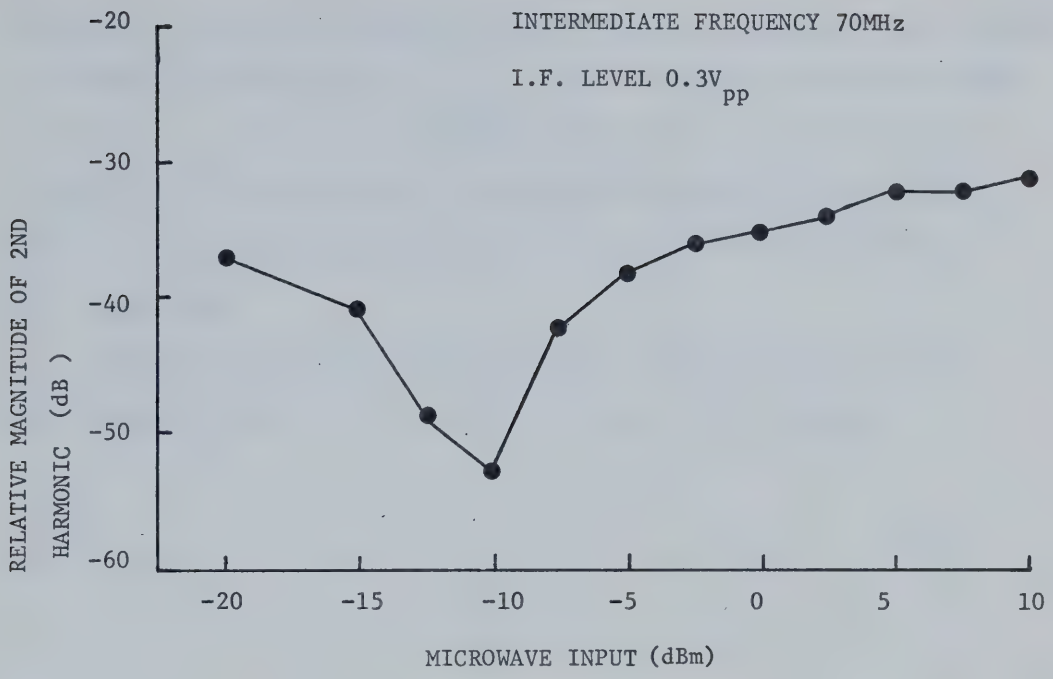

FIG. 4.17 RELATIVE MAGNITUDE OF SECOND HARMONIC VS. INPUT MICROWAVE LEVEL

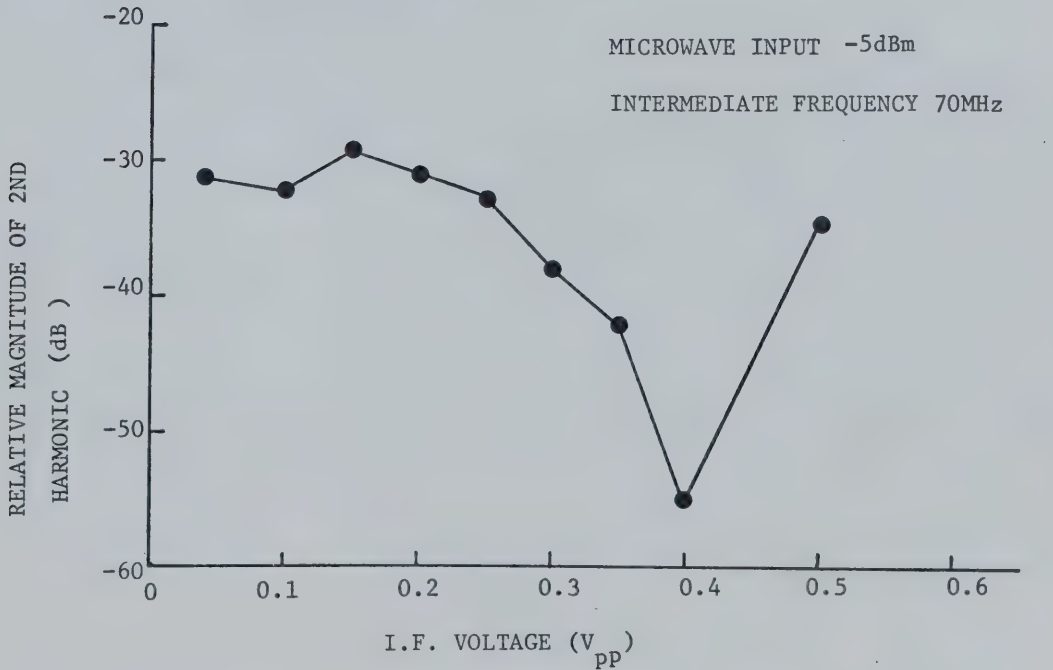

FIG. 4.18 RELATIVE MAGNITUDE OF SECOND HARMONIC VS. I.F. VOLTAGE LEVEL

amplitude of the second harmonic is plotted as a function of i.f. voltage. A minimum is observed at 0.4 V_{p-p}. Again the third harmonic was always more than below the fundamental. The results indicate that the distortion of the upconverter for amplitude modulated signals is very small. The second harmonic is seen to be always more than 30dB below the fundamental.

Similar tests could be performed for frequency modulated i.f., replacing the crystal detector with a frequency discriminator.

CHAPTER V

SUMMARY AND CONCLUSIONS

A simple theoretical analysis of amplifier upconverter characteristics was carried out using the device and the circuit admittance data. The analysis was done by considering that the bias current modulation due to applied i.f. signal causes the admittance of the device to vary. This causes the amplifier gain to vary and, therefore modulation of the output signal, when a signal with fixed level and frequency is applied at the input. One of the sidebands (usually first) can be filtered out as the output. The following conclusions can be drawn from the analysis and the experimental results of the Impatt-amplifier upconverter:

Large conversion gain of the order of 13dB could be obtained. Conversion gain (efficiency) is large for small r.f. inputs and it decreases with increasing level of input signal. The upconverted power output, however, is greater for larger microwave input signals. Therefore, a compromise has to be made, while selecting input power level, between the output power and the conversion efficiency.

Larger conversion gain can be obtained by an increase in i.f. signal level. At larger i.f. but small r.f. levels a shift in admittance characteristics may cause the output to decrease, for a fixed input microwave frequency. The centre frequency can be readjusted to get a larger sideband response.

With an increased level of microwave input signal the denominator vector $\vec{D}$ increases and the gain of the amplifier decreases. However, a larger microwave signal level allows a larger i.f. signal to be applied at the bias circuit before the upconverter becomes unstable.

Large sidebands with decreased conversion efficiency can be achieved at higher r.f. levels.

The Impatt-amplifier upconverter performance is similar to the amplifier characteristics. Therefore, better upconversion performance can be obtained by better amplifier design.

Some additional conclusions can be drawn from the experimental measurements on two Impatt-amplifiers.

The sideband magnitude depends upon the circuit response at the component frequencies. Either of the sidebands (LSB or USB), therefore, could have larger magnitude depending upon the gain characteristics of the amplifier, input microwave frequency and the intermediate frequency.

The sideband magnitude is maximum when both the sideband component and the centre frequency lie in the amplification band of the amplifier. For broadband upconversion characteristics, therefore, the amplifier should be very broadband.

The sideband magnitude depends upon the centre frequency gain, input power level and the d.c. bias current. An optimum selection of these parameters has to be made for maximum sideband power.

The bias modulation could also cause some frequency and phase modulation of the r.f. particularly at higher i.f. levels. This causes an increase in the sideband level and therefore contributes to the up-converted output.

Distortion introduced by the Impatt-amplifier upconverter in the audio signals amplitude modulated on i.f. is very small. Second harmonic is more than 30dB below the fundamental.

5.1 Suggestions for Further Work:

An exact study of upconversion phenomena in Impatt-amplifiers from admittance considerations should be possible by including the following effects:

1. The device susceptance variations with applied bias signal should be included in the analysis. An estimate of the complex constant relating admittance variations to the small signal i.f. level may be necessary.
2. The circuit response at the component frequencies plays an important role in determination of component magnitudes. The effects should be included in the analysis.
3. The nonlinearity of device admittance and its variation with bias signal may be characterised. It may be possible then to exactly predict the sideband response and the intermodulation products in the upconverter.
4. A study of distortion introduced by the upconverter, when the baseband signal is frequency modulated, is necessary to investigate the usefulness of Impatt-amplifier upconverters in microwave systems.

REFERENCES

[1] Grace, M.I., "Down Conversion and Sideband Translation using Avalanche Transit-time Oscillators," Proceedings of IEEE (Letters) Vol. 54, pp. 1570-1571, Nov. 1966.

[2] Clorfiene, A.S., "Self Pumped Parametric Amplification with an Avalanche Diode," Proceedings IEEE (Letters), Vol.54, pp. 1956-1957, Dec. 1966.

[3] Evans, W.J. and Haddad, G.I., "Frequency Conversion in Impatt Diodes," IEEE Transactions on Electron Devices, Vol. ED-16, No. 1, pp. 78-87, January 1969.

[4] Evans, W.J. and Haddad, G.I., "Sideband Generation in Avalanche Transit-time Diodes," Proceedings 1st Biennial Conference on Engineering Applications of Electronics Phenomena," Cornell University, Ithaca, N.Y., pp. 281-300, August 1967.

[5] Fakatsu, Y., "Parametric Effects in Microwave Read Avalanche Diode," IEEE Transactions on Electron Devices, ED-14, No. 5, pp. 251-259, May 1967.

[6] Hines, M.E., "Large Signal Noise, Frequency Conversion and Parametric Instabilities in Impatt Diode Networks," Proceedings I.E.E.E., Vol. 60, No. 12, pp. 1534-1548, December 1972.

[7] Shen, C.C., Melick, D., Sweet, A., MacKenzie, L.A., "Avalanche Diode Oscillators: Power, Efficiency, Impedance and Mixing Studies," Proceedings 1st Biennial Conference on Engineering Applications of Electronic Phenomena, Cornell University, Ithaca, N.Y., pp. 253-265, August 1967.

[8] Ahmed, M.J., "Avalanche-diode Amplifier Upconverter," Electronics Letters, Vol. 9, No. 21, pp. 490-491, 18th October, 1973.

[9] Kita, S. and Kanmuri, N., "Millimeter-wave Up-converter Using a Germanium Avalanche," Electronics and Communications in Japan, Vol. 53-B, No. 12, pp. 86-93, 1970.

[10] Kita, S., "Millimeter Wave Parametric Down-converter Using Silver Bonded Diode at Breakdown Region," Proceedings I.E.E.E. (Letters), Vol. 54, pp. 1499-1500, October, 1966.

[11] Fukatsu, Y. and Kato, H.," Frequency Conversion with Gain Through Sideband Locking of an Impatt-diode Oscillation," Proceedings I.E.E.E. (Letters), Vol. 57, pp. 342-343, March, 1969.

[12] Laton, R.W. and Haddad, G.I., "Characteristics of Impatt-diode Reflection Amplifiers," I.E.E.E. Transactions on Microwave Theory and Techniques, Vol. MTT-21, No. 11, pp. 668-680, November 1973.

[13] Rice, S.O., "Volterra Systems with more than one Input Port-Distortion in a Frequency Converter," Bell System Technical Journal, Vol. 52, No. 8, pp. 1255-1268, October, 1973.

[14] Hewlett-Packard Application Note No. 935 - Microwave Power Generation and Amplification Using Impatt Diodes.

[15] Johnston, R.L., Deloach, B.C. Jr., and Cohen, B.G., "A Silicon Diode Microwave Oscillator," Bell System Technical Journal, Vol. 44, pp. 369-372, February, 1965.

[16] Napoli, L.S. and Ikola, R.J., "An Avalanching Silicon Diode Microwave Amplifier," Proceedings I.E.E.E. (Corresp.), Vol. 53, pp. 1231-1232, Sept. 1965.

[17] Penfield, P., Jr., Rafuse, R.P., Varactor Applications, M.I.T. Press, Cambridge, 1962.

[18] Watson, H.A., Microwave Semiconductor Devices and Their Circuit Applications, McGraw-Hill Book Company, 1969.

[19] Read, W.T., "A Proposed High Frequency Negative Resistance Diode," Bell System Technical Journal, Vol. 37, pp. 401-446, March 1958.

[20] Greiling, Paul, T. and Haddad, G.I., "Large-signal Equivalent Circuits of Avalanche Transit-time Devices," I.E.E.E. Transactions on Microwave Theory and Techniques, Vol. MTT-18, pp. 842-853, November 1970.

[21] Scherer, Ernst, F., "Large-signal Operation of Avalanche diode Amplifiers," I.E.E.E. Transactions on Microwave Theory and Techniques, Vol. MTT-18, pp. 922-932, November 1970.

[22] Gewartowski, J.W. and Morris, J.E., "Active Impatt diode Parameters Obtained by Computer Reduction of Experimental Data," I.E.E.E. Transactions on Microwave Theory and Techniques, Vol. MTT-18, pp. 157-161, March 1970.

[23] Syrett, B. - Ph.D. Dissertation, Department of Electrical Engineering, University of Alberta, to be presented.

[24] Mansour, N. - Ph.D. Dissertation, Department of Electrical Engineering, University of Alberta, to be presented.